

# UC Irvine

## UC Irvine Previously Published Works

### Title

Characteristics and influence of biosmoke on the fine-particle ionic composition measured in Asian outflow during the Transport and Chemical Evolution Over the Pacific (TRACE-P) experiment

### Permalink

<https://escholarship.org/uc/item/1qg7f88x>

### Journal

Journal of Geophysical Research: Atmospheres, 108(D21)

### ISSN

0148-0227

### Authors

Ma, Y  
Weber, RJ  
Lee, Y-N  
et al.

### Publication Date

2003-11-16

### DOI

10.1029/2002jd003128

### Copyright Information

This work is made available under the terms of a Creative Commons Attribution License, available at <https://creativecommons.org/licenses/by/4.0/>

Peer reviewed

## Characteristics and influence of biosmoke on the fine-particle ionic composition measured in Asian outflow during the Transport and Chemical Evolution Over the Pacific (TRACE-P) experiment

Y. Ma,<sup>1</sup> R. J. Weber,<sup>1</sup> Y.-N. Lee,<sup>2</sup> D. A. Orsini,<sup>1</sup> K. Maxwell-Meier,<sup>1</sup> D. C. Thornton,<sup>3</sup> A. R. Bandy,<sup>3</sup> A. D. Clarke,<sup>4</sup> D. R. Blake,<sup>5</sup> G. W. Sachse,<sup>6</sup> H. E. Fuelberg,<sup>7</sup> C. M. Kiley,<sup>7</sup> J.-H. Woo,<sup>8</sup> D. G. Streets,<sup>9</sup> and G. R. Carmichael<sup>8</sup>

Received 1 November 2002; revised 13 May 2003; accepted 16 May 2003; published 4 November 2003.

[1] We investigate the sources, prevalence, and fine-particle inorganic composition of biosmoke over the western Pacific Ocean between 24 February and 10 April 2001. The analysis is based on highly time-resolved airborne measurements of gaseous and fine-particle inorganic chemical composition made during the NASA Transport and Chemical Evolution over the Pacific (TRACE-P) experiment. At latitudes below approximately 25°N, relatively pure biomass burning plumes of enhanced fine-particle potassium, nitrate, ammonium, light-absorbing aerosols, and CO concentrations were observed in plumes that back trajectories and satellite fire map data suggest originated from biomass burning in southeast Asia. Fine-particle water-soluble potassium ( $K^+$ ) is confirmed to be a unique biosmoke tracer, and its prevalence throughout the experiment indicates that approximately 20% of the TRACE-P Asian outflow plumes were influenced, to some extent, by biomass or biofuel burning emissions. At latitudes above 25°N, highly mixed urban/industrial and biosmoke plumes, indicated by  $SO_4^{2-}$  and  $K^+$ , were observed in 5 out of 53 plumes. Most plumes were found in the Yellow Sea and generally were associated with much higher fine-particle loadings than plumes lacking a biosmoke influence. The air mass back trajectories of these mixed plumes generally pass through the latitude range of between 34° and 40°N on the eastern China coast, a region that includes the large urban centers of Beijing and Tianjin. A lack of biomass burning emissions based on fire maps and high correlations between  $K^+$  and pollution tracers (e.g.,  $SO_4^{2-}$ ) suggest biofuel sources. Ratios of fine-particle potassium to sulfate are used to provide an estimate of relative contributions of biosmoke emissions to the mixed Asian plumes. The ratio is highly correlated with fine-particle volume ( $r^2 = 0.85$ ) and predicts that for the most polluted plume encounter in TRACE-P, approximately 60% of the plume is associated with biosmoke emissions. On average, biosmoke contributes approximately 35–40% to the measured fine inorganic aerosol mass in the mixed TRACE-P plumes intercepted north of 25°N latitude.

**INDEX TERMS:** 0305 Atmospheric Composition and Structure: Aerosols and particles (0345, 4801); 0322 Atmospheric Composition and Structure: Constituent sources and sinks; 0365 Atmospheric Composition and Structure: Troposphere—composition and chemistry; 0368 Atmospheric Composition and Structure: Troposphere—constituent transport and chemistry; **KEYWORDS:** atmospheric aerosol, biomass burning, particle chemical composition, Asian air quality

**Citation:** Ma, Y., et al., Characteristics and influence of biosmoke on the fine-particle ionic composition measured in Asian outflow during the Transport and Chemical Evolution Over the Pacific (TRACE-P) experiment, *J. Geophys. Res.*, 108(D21), 8816, doi:10.1029/2002JD003128, 2003.

<sup>1</sup>School of Earth and Atmospheric Sciences, Georgia Institute of Technology, Atlanta, Georgia, USA.

<sup>2</sup>Environmental Sciences Department, Brookhaven National Laboratory, Upton, New York, USA.

<sup>3</sup>Department of Chemistry, Drexel University, Philadelphia, Pennsylvania, USA.

<sup>4</sup>Department of Oceanography, University of Hawaii at Manoa, Honolulu, Hawaii, USA.

<sup>5</sup>Department of Chemistry, University of California, Irvine, Irvine, California, USA.

<sup>6</sup>NASA Langley Research Center, Hampton, Virginia, USA.

<sup>7</sup>Department of Meteorology, Florida State University, Tallahassee, Florida, USA.

<sup>8</sup>Center for Global and Regional Environmental Research, University of Iowa, Iowa City, Iowa, USA.

<sup>9</sup>Argonne National Laboratory, Argonne, Illinois, USA.

## 1. Introduction

[2] During February–April 2001, the NASA Global Tropospheric Experiment (GTE) mounted a two-aircraft (NASA Wallops P-3B and NASA Dryden DC-8) airborne research campaign to investigate Asian continental outflow. Measurements have shown that the magnitude of these emissions is sufficient to influence the composition of the global atmosphere. The experiment is referred to as Transport and Chemical Evolution over the Pacific (TRACE-P). TRACE-P objectives include: to identify the major pathways for Asian outflow over the western Pacific, to chemically characterize the outflow, and to estimate contributions from different emission sources, such as biomass burning, and fossil fuel combustion, with a high priority to chemically characterize the biomass/biofuel component of the Asian outflow [Jacob *et al.*, 2003]. In this paper we focus on the contribution of emissions from biomass and biofuel burning (collectively referred to as biosmoke) to the fine particles.

[3] The chemical composition of both trace gases and aerosol particles in anthropogenic plumes provides information on emission sources. For example, the particulate potassium ion ( $K^+$ ) is often a useful tracer for identifying biomass burning [Andreae, 1983]. This is because the combustion of plant matter, which contains  $K^+$  as a major electrolyte within its cytoplasm, releases large amounts of  $K^+$ -rich particles in the submicron size fraction [Cachier *et al.*, 1991; Gaudichet *et al.*, 1995], and contributions of soil-derived or sea-spray-derived  $K^+$  in the submicron aerosol is usually small. Elemental carbon associated with potassium has also been used as a tracer for biomass burning plumes [Andreae, 1983]. Specific trace gases can serve as tracers, including hydrogen cyanide (HCN), acetonitrile ( $CH_3CN$ ), carbon monoxide (CO) [Reiner *et al.*, 2001; Singh *et al.*, 2003], and methylchloride ( $CH_3Cl$ ) [Blake *et al.*, 1999]. For fossil fuel and urban emissions, sulfur dioxide ( $SO_2$ ) is a useful tracer where no volcanic influences exist.

[4] Speciation of particulate organic compounds is commonly used for source apportionment studies and has been used for identifying biomass burning emissions [Fang *et al.*, 1999; Fine *et al.*, 2002; Simoneit, 1999; Simoneit *et al.*, 1993, 1999], biogenic emissions [Kavouras and Stephanou, 2002; Kawamura and Sakaguchi, 1999; Kubátová *et al.*, 2002; Mazurek and Simoneit, 1998; Sakaguchi and Kawamura, 1994], and anthropogenic sources [Frazer *et al.*, 2002; Nolte *et al.*, 2002]. Since organic particle speciation typically requires large quantities of sample leading to long sample integrate times, this method cannot readily be applied to airborne measurements where fast sampling rates are necessary to resolve individual plumes. By using more readily available and rapidly measured gaseous and aerosol compounds, the airborne data from TRACE-P and ACE-Asia can be used to estimate contributions from various sources over a broad geographical region. However, these compounds generally provide less specificity on aerosol sources than is available from speciation of organic particles.

[5] The aim of this paper is: to investigate the contribution of biosmoke to the inorganic components of Asian fine particles, to determine the biosmoke sources, and to quantitatively estimate the contribution of biosmoke to the Asian plumes observed during TRACE-P and ACE-Asia. As part of this latter objective, we will gauge the usefulness of fine-

particle  $K^+/SO_4^{2-}$  molar ratios for estimating relative contributions of biosmoke in urban plumes containing mixtures of pollution and biosmoke. This ratio may be especially useful since it is based solely on fine-particle ionic composition and is thus more readily measured than some gases and organic aerosol compounds.

[6] This study is unique in that we employ high-resolution data obtained from the Particle-Into-Liquid Sampler coupled to Ion Chromatographs (PILS-IC), for rapid and automated measurements of the aerosol particle bulk ionic composition. Fast measurements of aerosol ionic composition not only provides a larger data set but also is capable of distinguishing variability within a plume, and plumes of different composition in close proximity. Previous studies have used integrated filter methods, whose application to airborne plume studies through the use of tracers (biomass burning/pollution) is often restricted by the long sampling integration times and poor resolution during vertical profile flights.

## 2. Experimental Procedure

[7] The TRACE-P experiment focused mainly on eastern Asia and the western Pacific Basin. Both research aircraft, the DC-8 (ceiling 12 km) and the P-3B (ceiling 7 km) were operated first out of Hong Kong, P. R. China (22.3°N, 113.92°E) and then the Yokota Air Force Base, Japan (35.76°N, 139.92°E) from February to April 2001. These two bases of operations were well situated to sample Asian outflow over the range of latitudes from 10°N to 50°N. The payload of the two aircraft included a suite of instruments for measurements of both atmospheric gases and aerosols, and meteorological parameters. This analysis uses mainly the P-3B high-time-resolution particle composition data. The regions investigated by this aircraft during the intensive field study of 4 March to 4 April were mainly within the area of 5°–45°N, 110°–155°E. The following analysis focuses only on this region. Data from the transit flights from North America to Asia and back are not included.

[8] Following the TRACE-P study, the National Science Foundation's (NSF) Asian Aerosol Characterization Experiment (ACE-Asia) also performed airborne measurements in the same region from 31 March to 4 May [Huebert *et al.*, 2003]. Identical instrumentation for the measurement of some compounds were deployed on the NSF C-130 research aircraft, including measurements of fine-particle inorganic composition, light-absorbing aerosols, and sulfur dioxide. Selected data from this study are also discussed in this paper.

[9] A Particle-Into-Liquid Sampler coupled to Ion Chromatographs (PILS-IC) measured fine aerosol inorganic chemical composition on the P-3B. In this instrument, sample air is first drawn through denuders to remove interfering gases and then adiabatically mixed with saturated water vapor. In this environment, sampled ambient particles grow to sizes that are easily captured by inertial impaction onto a small wetted area. With the addition of a small ( $\sim 0.1$  ml/min) transport flow, the resulting liquid flow containing the water-soluble aerosol components is then analyzed on-line and continuously with anion and cation ion chromatography. The chosen analysis method permits a

4 min duty cycle for measurements of  $\text{Na}^+$ ,  $\text{Na}_4^+$ ,  $\text{Ca}^{2+}$ ,  $\text{K}^+$ ,  $\text{Mg}^{2+}$ ,  $\text{Cl}^-$ ,  $\text{NO}_3^-$ , and  $\text{SO}_4^{2-}$ . The PILS-IC deployed for this mission had an upper size measurement limit (50% efficiency) at  $1.3\ \mu\text{m}$  aerodynamic diameter. Limits of detection vary for specific species, but are approximately  $10\ \text{ng m}^{-3}$  (3 pptv) for the anions and  $50\ \text{ng m}^{-3}$  (45 pptv) for cations. A more detailed instrument description is given in Weber *et al.* [2001] and Orsini *et al.* [2003]. An intercomparison of the PILS-IC to various other measurement techniques during this mission and ACE-Asia is discussed elsewhere [Ma *et al.*, 2003].

[10] During sampling, ram air heating and heat transfer from the cabin to the sample during transport to the instrument can result in loss of semivolatile aerosol components. For ionic components, this is most likely to result in an undermeasurement of nitrate and the ammonium that is associated with the nitrate. Measurements of the difference between sample and ambient temperatures were typically about  $10^\circ\text{K}$  at low altitudes and about  $35^\circ\text{K}$  at higher altitudes making the volatility losses most severe during higher altitude measurements. Particle losses during the transmission are estimated at approximately 2% for  $1\ \mu\text{m}$  particles.

[11] Nonmethane hydrocarbons and other trace gases were measured in whole air samples collected by the University of California-Irvine (UCI). Stainless steel canisters of 2 L are pressurized by a two-stage metal bellows pump and then ferried to UCI for analysis via gas chromatography. The measurement precision for  $\text{CH}_3\text{Cl}$  was 2% and for tetrachloroethene ( $\text{C}_2\text{Cl}_4$ ) was 2% or 0.05 pptv, whichever is larger. A more detailed method description is given in Sive [1998].

[12] A continuous light absorption photometer (PSAP-Radiance Research) was used to alternatively quantify the light absorption coefficient of all particles and particles smaller than  $1\ \mu\text{m}$  aerodynamic diameter at 565 nm wavelength by the University of Hawaii. Size selection was obtained by switching an inertial impactor on or off line. The PSAP records changes in optical transmission through a filter onto which particles are continually collected. Filter absorption is then related to the optical absorption coefficient using Beer's law and a calibration coefficient [Bond *et al.*, 1999]. The fine-particle volume concentration was also measured by the University of Hawaii research group with a custom-made Laser Optical Particle Counter (OPC) [Clarke, 1991].

[13] Fast response tunable diode laser sensors measured carbon monoxide spectroscopically. The DACOM (Differential Absorption CO Measurement) instrument had a time resolution of 1 s [Sachse *et al.*, 1991]. Sulfur dioxide was measured with Atmospheric Pressure Ionization Mass Spectrometry (APIMS) with an average time resolution of 1 s [Thornton *et al.*, 2002]. This technique involves a quadrupole mass spectrometer with a nickel-63 (Ni-63) source. High isotopic purity S-34  $\text{SO}_2$  is added to the ambient air as an internal standard.

[14] Because the time resolution of the various measurement techniques differs, 4 min averaged data files merged according to the PILS were generated by NASA Langley Research Center and used for the analysis. The data set can be accessed through the GTE website at <http://www-gte.larc.nasa.gov>.

[15] Five day back trajectories, generated by Florida State University, are also used in our analysis. The trajectories are calculated using a kinematic model employing wind components from the European Center for Medium Range Weather Forecasts (ECMWF). The data have  $1.0^\circ \times 1.0^\circ$  horizontal resolution, 61  $\sigma$  levels (terrain following coordinate system) in the vertical, and are available at 6 hour intervals throughout the TRACE-P period. Additional details on the trajectory model, along with a comparison between kinematic and isentropic trajectories, are given in Fuelberg *et al.* [1996].

[16] The University of Iowa research group provided modeling estimates of daily emissions from biomass burning for CO, black carbon (BC) and other species using AVHRR data provided from the World Fire Web (WFW), (<http://www.gvm.jrc.it/tem/wfw/wfw.htm>) and TOMS Aerosol Index data (<http://toms.gsfc.nasa.gov/aerosols/aerosols.html>). Emissions from biomass burning were estimated only for field combustion, which includes burning of forest, savanna, and agricultural residues. First, total emissions are estimated based on the emission database from Argonne National Laboratory. World Fire Web data are used for determining the spatial and temporal (daily) emissions, and TOMS-Aerosol Index (AI) is used to reduce both cloud interference and satellite coverage limitations. Emission factors for each species are then estimated by dividing the total emission by total fire count. The daily emission of each species is derived by multiplying emission factors by daily AI-adjusted fire counts. More details about the methodology of emission database and biomass burning estimation are given in Streets *et al.* [2003] and Woo *et al.* [2003].

### 3. Results and Discussion

[17] We begin our analysis of biosmoke emissions recorded during TRACE-P by first characterizing a well-defined plume that was clearly of biomass burning origin. Plumes of mixtures of biosmoke and pollution are then investigated.

#### 3.1. Characteristics of a Relatively Pure Biomass Burning Plume, Flight 10

[18] The purest biomass burning plume recorded during TRACE-P was measured north of the Philippines in the Luzon Strait during P-3B flight 10 on 9 March 2001 0258–0346 UTC. The source of this plume is consistent with back trajectories and fire maps of biomass burning regions. Estimates of the spatial distribution of biomass burning CO and black carbon emissions averaged over 5 days prior to the flight are shown in Figure 1. These emissions are calculated based on the method described in the experiment section above. Five day back trajectories that arrived along the flight track are also shown in Figure 1. A plume that was measured near 3 km above sea level (asl) shows that the air originated from the region of Southeast Asia. Five days prior to this flight, this region experienced extensive biomass burning, most of which appears to be from Thailand where the vegetation is mainly savanna grassland and tropical forest. Surface-level back trajectories, also shown in Figure 1, indicate that these air masses did not intercept the biomass burning region, but instead they may have originated from the vicinity of Hanoi.

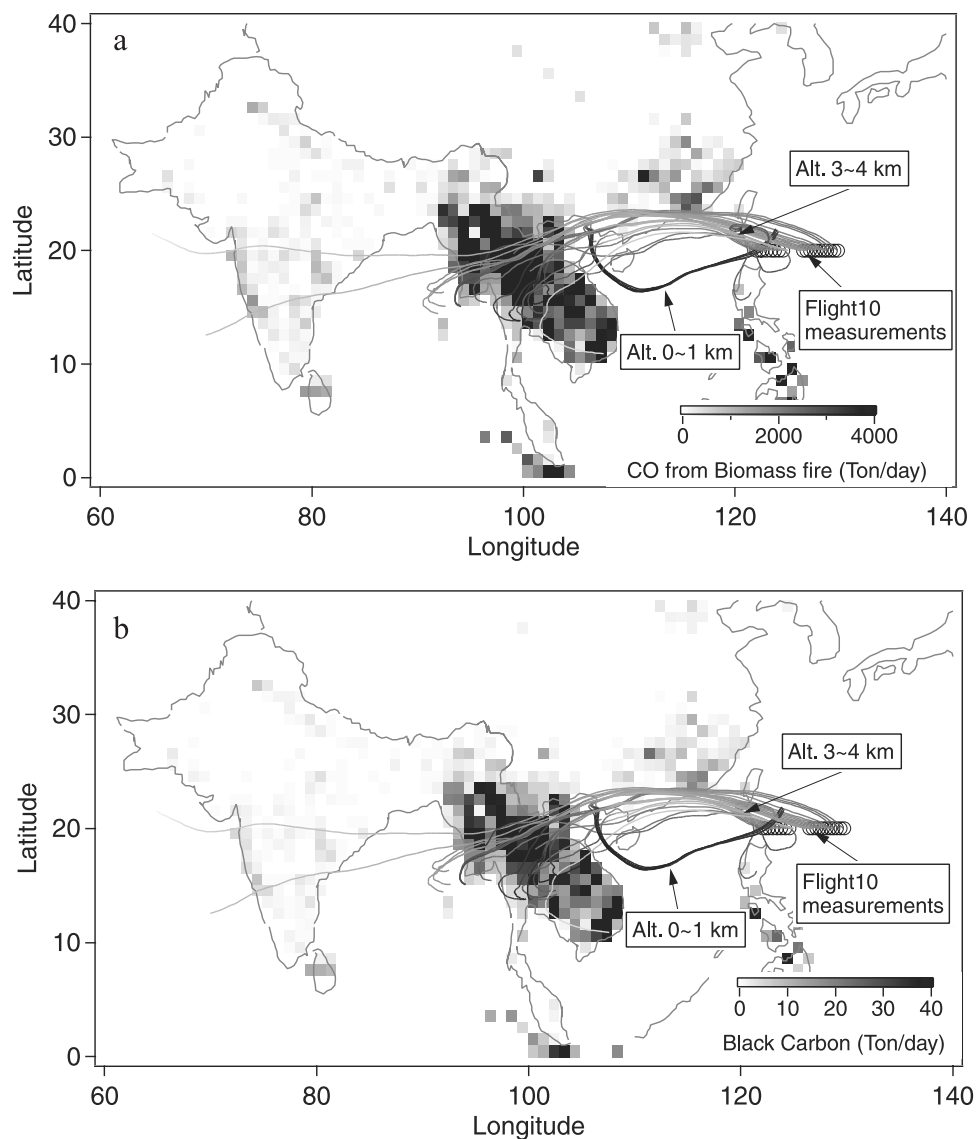


**Figure 1.** Spatial distribution of (a) biomass burning CO and black carbon emissions averaged over 5 days prior to TRACE-P P-3B flight 10 and (b) 5 day back trajectories for the plumes encountered during flight 10.

[19] Aircraft altitude, relevant gases, and fine-particle ionic concentrations measured in the region where the biomass burning plume was detected are shown in Figure 2. These measurements include a number of soundings and level leg runs. The sounding measurements are used to construct the vertical profiles in Figure 3. On the basis of fine-particle concentrations of  $K^+$  and  $SO_4^{2-}$ , a temperature inversion at approximately 2.2 km asl ( $T$  is not plotted) appears to separate a biomass burning layer near 3 km asl (high  $K^+$ ) from a surface-level pollution layer (high  $SO_4^{2-}$ ), consistent with the back trajectories. In both Figures 2 and 3, various fine-particle components are associated preferentially in one of the two plumes, and some species are found in both. However, CO and absorbing particles are found in both layers, and both are the highest in the biomass burning plume.  $CH_3Cl$  is the highest in the biomass burning plume. On average, the  $K^+$  concentration in the 3 km asl plume is 700 pptv and near zero in the surface plume.  $NO_3^-$  has the

same trend as  $K^+$  and reaches its highest concentration of more than 1000 pptv, also at 3 km asl. Smaller amounts of  $NO_3^-$  are also observed in the pollution layer. In contrast,  $SO_4^{2-}$ , which is apparently not produced in significant amounts during biomass burning [Chin *et al.*, 1996], shows a small increase at 3 km, possibly due to some mixing of pollution with the biomass burning plume or from background  $SO_4^{2-}$  that was present upwind of the biomass burning region. Sulfate concentrations are clearly highest in the surface pollution layer. Ammonium is found in both plumes, however the highest concentrations of ammonium are observed in the upper biomass burning plume. Although not plotted,  $Ca^{2+}$  and  $Na^+$  are both less than 100 pptv at 3 km asl suggesting little influence from fine mineral dust or fine sea salt in this region.

[20] For the ionic measurements within the biomass burning plume (altitude  $> 2$  km asl),  $K^+$  is highly correlated with  $NO_3^-$ ,  $NH_4^+$ , and  $SO_4^{2-}$ , all with  $r^2$  higher than 0.9. In



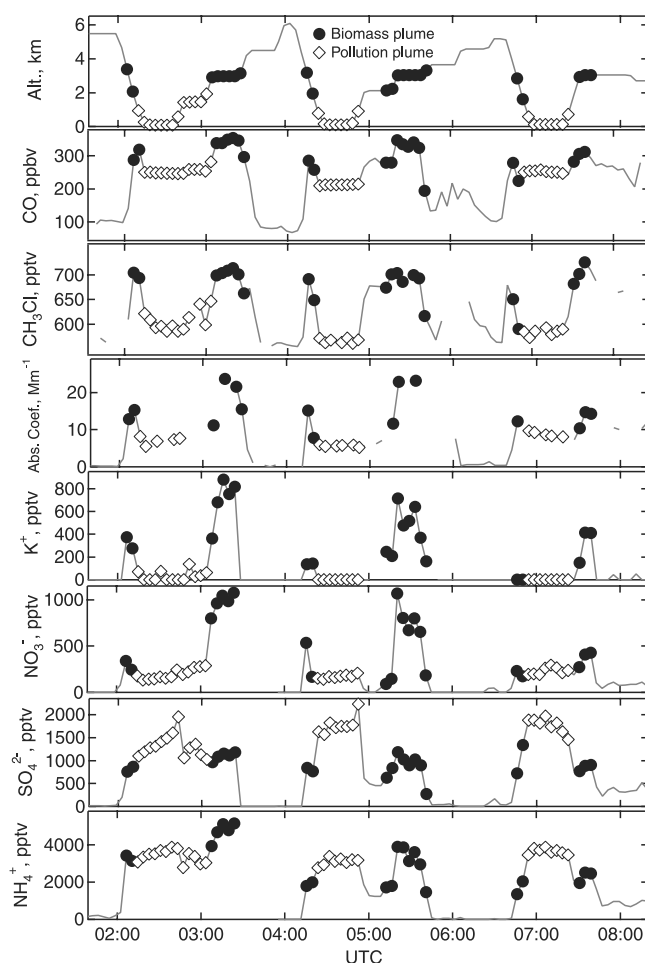


**Figure 2.** Aircraft altitude, relevant gases, and fine-particle ionic concentrations measured during P-3B flight 10 in a relatively pure biomass burning plume from Thailand.

the boundary layer pollution plume (altitude < 2 km asl),  $\text{NH}_4^+$  correlates with  $\text{SO}_4^{2-}$ ,  $r^2 = 0.80$ , but shows no correlation with  $\text{K}^+$  or  $\text{NO}_3^-$ .

[21] The vertical profiles based on two soundings are shown in Figure 3 along with the fine-particle ion balance. Throughout the study,  $\text{NH}_4^+/\text{SO}_4^{2-}$  molar ratios were typically near 2, as observed in the surface-level pollution plume. However, in the biomass burning plume, the ratio varies from 2 to 6. Considering all the ions measured for all TRACE-P research flights, the positive/negative charge ratio is on average 0.92 (excluding data from volcanic plumes), suggesting that the PILS-IC captures most of the aerosol ionic components. The ionic balance ( $\sum \text{cations} - \sum \text{anions}$ , in equivalents) in Figure 3 shows that additional anions were not measured in the biomass burning plume. The ratio of ion difference/total ions reaches as high as 27%. These missing anions are likely organic acids not measured, but associated with the biomass burning plume [Tabazadeh *et al.*, 1998].

[22] Although fine organic aerosol particle mass was not measured, comparisons between the sum of the PILS ionic mass and optical particle measurements of fine-particle

volume show that in the biomass burning plume, the fraction of ionic mass to fine volume was significantly less than other plumes, consistent with expectations of large concentrations of organic species in the biomass burning plume.

[23] Similar results were observed in flight 9, a flight sampling in the same region 2 days prior to flight 10. All together, these measurements confirm previous findings that biomass burning plumes are significant sources of CO, light-absorbing particles (element carbon, EC), and fine water-soluble  $\text{K}^+$ ,  $\text{NO}_3^-$ ,  $\text{NH}_4^+$  (and organic carbon, but this was not measured), and generally minor sources of sulfur compounds such as  $\text{SO}_4^{2-}$ . Our analysis uses these unique sources for these various species to identify and delineate biosmoke and pollution contributions in the Asian plumes.

### 3.2. Correlations of Biosmoke Tracers and Tracer Spatial Distributions

[24] Compounds such as CO,  $\text{CH}_3\text{Cl}$ , light-absorbing particles, and  $\text{K}^+$ , were detected in many of the plumes encountered during TRACE-P. Here we focus on fine water-soluble  $\text{K}^+$  as a biosmoke tracer since it appears to be uniquely associated with biosmoke. To test if this applies to the complete TRACE-P data set, correlations between  $\text{K}^+$  and known biosmoke burning indicators are investigated through linear regressions.

[25] Elemental carbon (EC) is one major product of biomass burning. In this analysis, we use the aerosol light absorption coefficient as a surrogate for EC. Other absorbing aerosols, such as mineral dust, can also contribute to this measurement. However, based on PILS measurements of soluble calcium concentrations, mineral dust contributions were generally minor. For the data collected during all intensive TRACE-P research flights,  $\text{K}^+$  is correlated with the absorption coefficient with an  $r^2$  of 0.73, shown in Figure 4a. Because higher concentrations can exert a disproportionate effect on the linear regression, a plot is also made for those  $\text{K}^+$  concentrations less than 1000 pptv, shown in the smaller plot of Figure 4a, for this data, the  $r^2$  is 0.66. Incomplete combustion is a global source for CO, whether from wildfires or fossil fuel burning. Similar to the relationship between  $\text{K}^+$  and absorption coefficient,  $\text{K}^+$  is also correlated with CO with an  $r^2$  of 0.61 for all TRACE-P research flight data; for  $\text{K}^+$  concentrations less than 1000 pptv, the  $r^2$  is 0.44 (Figure 4b). The positive nonzero intercept in both the absorption coefficient (EC) and CO versus  $\text{K}^+$  plots is likely due to EC and CO sources are not associated with biosmoke.

[26] Although  $\text{CH}_3\text{Cl}$  is also used as a biomass burning tracer, in this study the overall correlation between  $\text{CH}_3\text{Cl}$  and  $\text{K}^+$  is not as high as expected. For the lower latitude (south of  $25^\circ\text{N}$ ) measurements where biomass burning influences are greatest, the correlation between  $\text{K}^+$  and  $\text{CH}_3\text{Cl}$  is  $r^2 = 0.49$ . For specific plumes containing mixed biosmoke and pollution,  $\text{K}^+$  and  $\text{CH}_3\text{Cl}$  correlations are relatively high (e.g.,  $r^2$  typically between 0.4 and 0.7). However, due to the differences in  $\text{CH}_3\text{Cl}$  background concentrations and the variation in  $\text{K}^+$  versus  $\text{CH}_3\text{Cl}$  slopes for different plumes, the overall combined  $r^2$  is low at 0.28. The low correlation between  $\text{CH}_3\text{Cl}$  and other biomass burning tracers is also discussed in Heald *et al.* [2003].

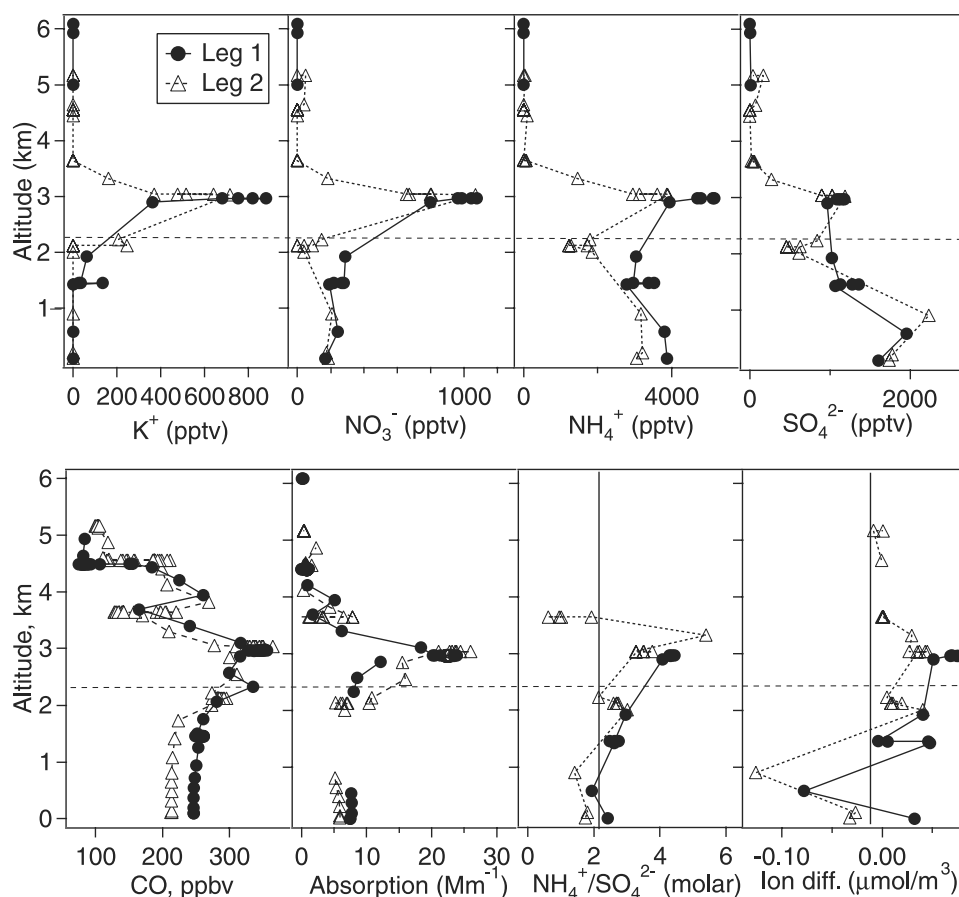


**Figure 3.** Vertical profiles for various species measured in the region of the biomass burning plume of P-3B flight 10. Closed circles are for leg 1 and open triangles are for leg 2. A temperature inversion at  $\sim 2$  km asl separates the biomass burning plume from a surface-level pollution layer.

Differences in  $K^+/CH_3Cl$  slopes may be caused by interferences from natural production of  $CH_3Cl$  from Asian sources other than biomass burning [Lee-Taylor *et al.*, 2001] or differences in the physical-chemical properties of  $K^+$  and  $CH_3Cl$ .  $CH_3Cl$  is a fairly long-lived gas (approximately 1 year), while  $K^+$  is water-soluble and readily scavenged by precipitation. However, differences in physical-chemical properties would also result in poor  $K^+/CO$  correlations, which was not the case.

[27] Fine-particle  $K^+$  is correlated with fine-particle ammonium ( $NH_4^+$ ) in the biomass burning plume of flight 10 (Figures 2 and 3) and this correlation is strong for all TRACE-P data; the  $K^+ - NH_4^+ r^2 = 0.77$  and  $0.51$  when  $K^+$  is lower than  $1000$  pptv, Figure 5. Other studies have also shown that biomass burning can be a source of  $NH_3$  leading to fine-particulate [Andreae and Merlet, 2001]. Although  $NO_3^-$  was also found in the “pure” biomass plumes, it is not as highly correlated to  $K^+$  for all the TRACE-P data, where the  $r^2$  is  $0.67$ . This suggests that other large sources, such as urban/industrial regions are also high  $NO_3^-$  sources and further support the unique and significant biosmoke source for  $K^+$  and  $NH_4^+$  during TRACE-P.

[28] The correlations based on all TRACE-P data collected in Asia suggest that  $K^+$  is a good tracer for biosmoke. Fine-particulate  $K^+$  was observed throughout the experi-

ment. The spatial distribution measured by the P-3B during TRACE-P within the western Pacific is shown in Figure 6a. Peak concentrations are found at both high and low latitudes, and maximum concentrations are found between  $120^\circ$  and  $130^\circ E$  longitude. The vertical  $K^+$  profile in Figure 6b shows that concentrations are generally the highest near the surface. The peak of approximately  $1000$  pptv at  $3$  km asl was the flight 10 “pure” biomass burning plume discussed above. For latitudes above  $25^\circ N$ , highest  $K^+$  concentrations are observed near the ocean surface, mainly in the Yellow Sea, and low concentrations are generally observed east of Japan. It will be shown that backward air trajectories for most of the regions of high  $K^+$  pass through the latitude range of  $34^\circ$  and  $40^\circ N$ , on the eastern China coast, and are mixed with urban/industrial emissions. In the following section, we present detailed results from two urban plumes that contain  $K^+$ . The first is a Yellow Sea plume of maximum  $K^+$  measured during TRACE-P (P-3B flight 14). For comparison, the second is a mixed plume of low  $K^+$  observed in the Sea of Japan (P-3B flight 19). Both plumes are identified in Figure 6a.

### 3.3. Case Studies of Mixed Biosmoke/Pollution Plumes

#### 3.3.1. Case 1: P-3B Flight 14, Yellow Sea

[29] The plume encountered in the Yellow Sea on P-3B flight 14 is unique in that it contained the highest  $K^+$

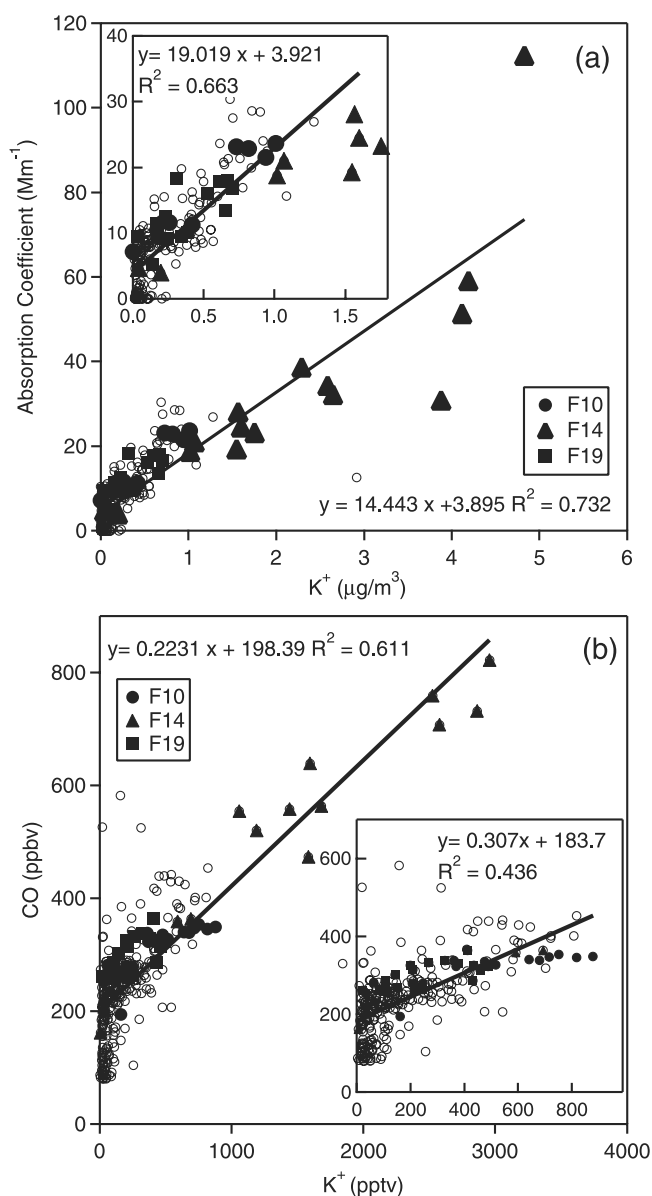


**Figure 4.** Relationship between water-soluble fine potassium and (a) light-absorbing aerosol particles (PSAP measurement) and (b) CO for all intensive flights shown in Figure 1. The insert is for potassium less than 1000 pptv. The data for the three case studies are highlighted. The data for the three specific flights are highlighted.

concentrations recorded during TRACE-P and ACE-Asia. These  $K^+$  concentrations are also higher than those recorded during the Pacific Exploratory Mission in the western Pacific, phase A in 1991, and B in 1994 (PEM-West A & B) where maximum concentrations were 241 pptv and 260 pptv, respectively [Dibb et al., 1997].

[30] Many other species in the plume were also unusually high, including the fine-particle absorption coefficient (likely mainly EC since there is little mineral dust), CO,  $NH_4^+$ ,  $NO_3^-$ ,  $SO_4^{2-}$ , and  $SO_2$ ; all species reach the highest concentrations of TRACE-P. Measurements in this plume are identified in the scatter plots of Figures 4 and 5. Peak concentrations were 3.0 ppbv ( $4.7 \mu g/sm^3$ ) for  $K^+$ , 23.2 ppbv ( $16.9 \mu g/sm^3$ )

for  $NH_4^+$ , 15.9 ppbv ( $40.2 \mu g/sm^3$ ) for  $NO_3^-$ , and 6.1 ppbv ( $24.1 \mu g/sm^3$ ) for  $SO_4^{2-}$ . The total ionic mass concentration reached  $88.9 \mu g/sm^3$  ( $sm^3$  means standard cubic meters, where standard conditions are  $T = 25^\circ C$  and a pressure of 1 atmosphere).

[31] During the measurements in the Yellow Sea, the plume was intercepted in the two surface legs below 1 km asl in two different positions ( $29.9^\circ$ – $33.0^\circ N$  and  $33.7^\circ$ – $36.0^\circ N$  latitude) during north and southbound legs. The ionic composition of the plume is shown in Figure 7. The correlation ( $r^2$ ) between  $K^+$  and  $SO_4^{2-}$  in the two passes is 0.72, suggesting strong mixing of biosmoke and fossil fuel combustion. The  $NH_4^+/SO_4^{2-}$  molar ratio reaches up to approximately 4–5 within the plume, but the measured ions are nearly in a charge balance. The average ratio of the sum of cations minus sum of anions to total ions measured (molar ratio) is less than 2%. This plume is also atypical in that  $NO_3^-$  exceeds  $SO_4^{2-}$ .  $NO_3^-/SO_4^{2-}$  molar ratios typically range between 0 and 1 for the study, however, in this plume the ratio reached 3, which is the highest of TRACE-P. We note that nitrate was also observed in the pure biomass burning plume of flight 10 and might also be associated with the biosmoke in this plume. Near complete ion balance between  $SO_4^{2-}$  plus  $NO_3^-$  and  $NH_4^+$  suggests that most of it is likely  $NH_4NO_3$ .

[32] On the basis of fine-particle water-soluble calcium, Figure 7 shows that there was also some dust present in the plume; calcium concentrations were on average 800 pptv. Relative to the total molar mass of all ions,  $Ca^{2+}$ , however, comprised on average only 2%. There is little influence from fine sea salt since PILS  $Na^+$  concentrations are less than 500 pptv in the plume. The 5 day backward trajectories that arrived along the boundary layer flight track, the spatial distributions of CO and black carbon biomass burning emissions averaged over the previous 5 days prior to the

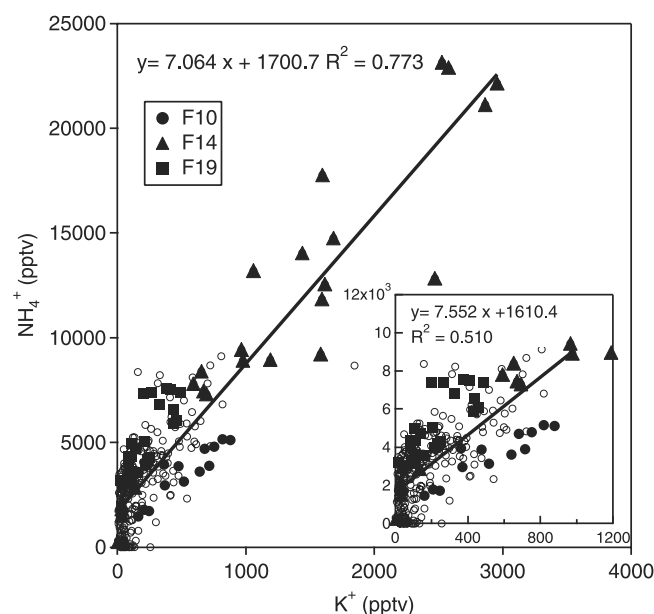


**Figure 5.** Relationship between water-soluble fine potassium and ammonium for all intensive flights shown in Figure 1. The insert is for potassium less than 1000 pptv. The data for the three case studies are highlighted. The data for the three specific flights are highlighted.



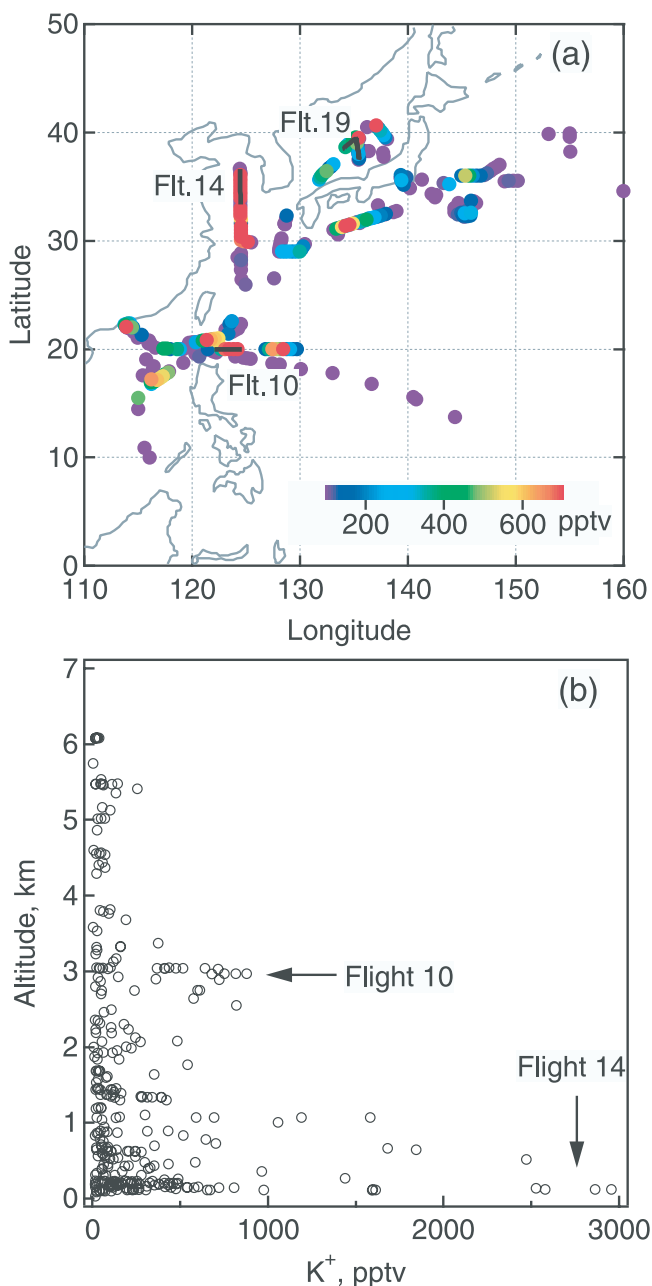


**Figure 6.** (a) Spatial distribution and (b) vertical distribution of water-soluble fine-particle potassium measured on the NASA P-3B aircraft in the western Pacific during TRACE-P. The locations of three specific plumes discussed in detail are also shown in Figure 6a as bold lines.

flight, and urban/industrial emissions of  $SO_2$  and  $NO_x$  for year 2000 are shown in Figure 8. Biomass burning emissions are based on the model predictions of *Woo et al.* [2003] and the pollutant emissions on the inventory of *Streets et al.* [2003]. Back trajectories for the plume in two legs suggest they originated from the same region and followed similar trajectories to the point where measured. Arriving from the northwest midtroposphere, the air masses subsided to the surface in the China coastal region, swinging westerly then moving easterly over the Yellow Sea

where they are intercepted by the aircraft (Figure 8). The trajectories cross a number of urban regions at about 2 km altitude, including Beijing and Tianjin. The observed dust ( $Ca^{2+}$ ) may be from mixing with higher altitude air originating from the more arid regions of Mongolia and Russia, or more localized sources of  $Ca^{2+}$  associated with the urban regions (e.g., cement production, construction, etc). Approximately 1% of  $Ca^{2+}$  was from sea salt based on  $Ca^{2+}$  and  $Na^+$  concentrations and their molar ratio in seawater.

[33] This plume may have been heavily influenced by biofuel combustion in urban regions, such as Beijing, and when added to urban pollutants may explain why this was the most polluted plume encountered in TRACE-P. It is noted that the predicted biomass burning black carbon and CO emissions shown in Figure 8 are about an order of magnitude lower in the possible source regions of this plume compared to those that contributed to the biomass burning plume of flight 10, shown in Figure 1. However, measured concentrations of CO and light-absorbing fine particles, and other species associated with biosmoke are much higher in the Yellow Sea plume. It may be that this plume is much closer to the source, is fresher, and thus less diluted. Given that the biomass burning tracers ( $K^+$ , CO) are well mixed with pollution tracers ( $SO_4^{2-}$ ), a more likely explanation is that this plume is from biofuel combustion in the region, or open burning within or near the city, instead of widespread biomass burning of forest or agriculture residue. Although biofuel burning is estimated to account for less than 10% of the total global emission of  $K^+$  [Andreae and Merlet, 2001], in China, roughly 30% of the fuel consumed is from the use of biofuel [Singh et al., 2003]. These emissions are not shown in Figure 8. Urban biofuel emissions combined with large anthropogenic sources of  $SO_2$  and  $NO_x$ , could lead to the observed high levels of ammonium sulfate and nitrate salts, and  $K^+$ . Alternatively, an unusually large industrial source for  $K^+$  in this region cannot be ruled out, but seems unlikely. It is also unlikely that the  $K^+$  is due to long range transport of biomass burning emissions from lower latitudes since the longer range back trajectories intercepting the Yellow Sea region do not dip south where extensive biomass burning occurs; instead, the trajectories come from a northwest direction (see Figure 8).

### 3.3.2. Case 2: P-3B Flight 19, Sea of Japan Mixed Biosmoke/Pollution Plume

[34] A fairly large plume was also intercepted in the Sea of Japan (Figure 6) during flight 19 and is apparently also a mix of biosmoke and pollution emissions based on  $K^+$  and  $SO_4^{2-}$  concentrations. The ionic composition of the plume is shown in Figure 9.  $K^+$  and  $SO_4^{2-}$  are also correlated in this plume, ( $r^2 = 0.61$ ) suggesting the sources are well mixed. The molar ratio ranges between 2 and 3, the  $NO_3^-/SO_4^{2-}$  ratio is between 0.5 and 1, which is more typical of the plumes measured during TRACE-P. Much of the could be  $NH_4NO_3$  since the average ratio of  $NH_4^+/(SO_4^{2-} + NO_3^-)$  in equivalence is 0.91. The measured ions also tend to be in charge balance. The ratio of the charge imbalance to total ion concentration is less than 1%. Similar to the Yellow Sea plume, backward trajectories arriving along the flight track in the boundary layer, Figure 10, suggest that the plumes are mainly from low altitudes apparently having passed over northeast and eastern coastal regions in China, and along the

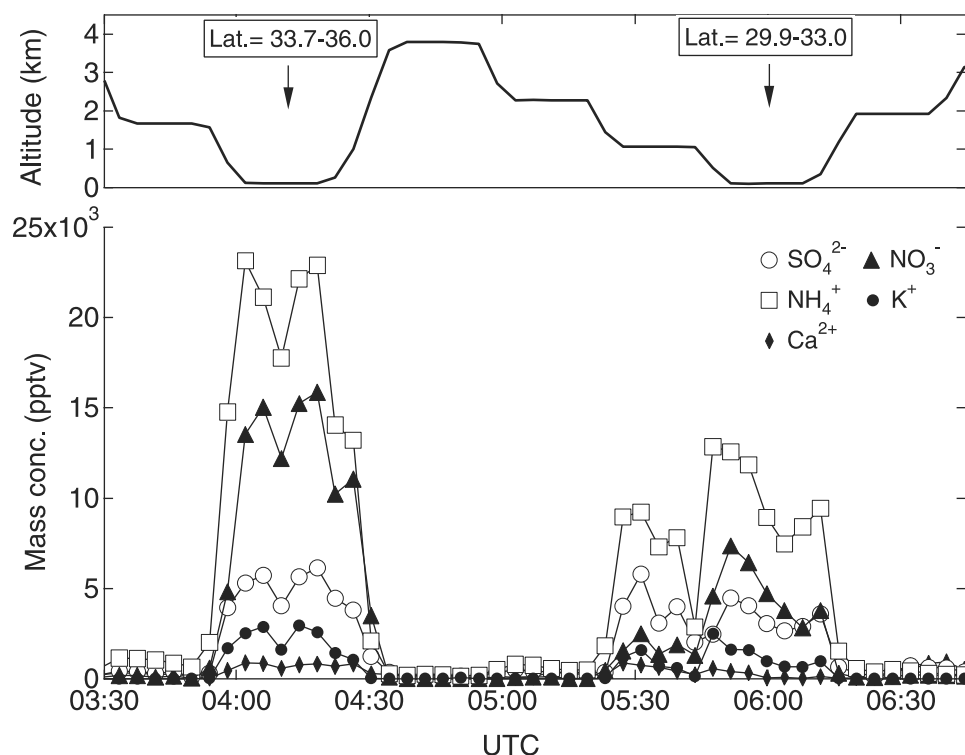


**Figure 7.** Aircraft altitude and fine-particle ionic composition in the Yellow Sea plume of P-3B flight 14. The plume was intercepted twice in the boundary layer at different locations.

west coast of the Yellow Sea. The air masses then moved over the Yellow Sea, South Korea, and entered the Sea of Japan where it was intercepted.

[35] These trajectories suggest that much of the observed pollutants may have also originated from China but were transported farther distances than the Yellow Sea plume. This is consistent with an estimate of plume age based on the ratio of  $\text{SO}_4^{2-}/(\text{SO}_2 + \text{SO}_4^{2-})$ . The use of this ratio as a measure of plume age is only valid if the plumes did not undergo cloud processing prior to detection. The  $\text{SO}_4^{2-}/(\text{SO}_2 + \text{SO}_4^{2-})$  ratio for the Yellow Sea flight 14 is 0.4, and for the Sea of Japan flight 19 plume is 0.5 pptv/pptv (see Table 2), consistent with it being more aged based on the ratio of  $\text{C}_2\text{H}_2/\text{CO}$ . On the basis of back trajectories, the pure biomass burning plume of flight 10 apparently had traveled the longest distance, and the ratio of  $\text{SO}_4^{2-}/(\text{SO}_2 + \text{SO}_4^{2-})$  in this case is 0.89 pptv/pptv, significantly higher than those from flight 14 and flight 19.

### 3.4. Observations of Biosmoke From Other Trace-P Aircraft and During the ACE-Asia Experiment

[36] Many of the unique characteristics recorded in these plumes have also been observed several times during the TRACE-P and ACE-Asia studies. When the other TRACE-P research aircraft (DC-8) sampled in the Yellow Sea on 10 March 2001, (0500–0530 UTC, DC-8 flight 9), 8 days prior to the P-3B flight 14, a similar aerosol chemical composition was observed. Integrated filter measurements by the University of New Hampshire recorded high concentrations of  $\text{NH}_4^+$  and  $\text{K}^+$ , and molar ratios of  $\text{NO}_3^-/\text{SO}_4^{2-}$  exceeded 1 [Jordan et al., 2003]. Five day back trajectories also show a similar pattern as the P-3B flight 14 discussed in case one; in both cases trajectories originate from the

northwest and subside to the boundary layer in the China coastal region of the Yellow Sea and then move to the east.

[37] Approximately 1 month following the TRACE-P measurements, the C-130 research aircraft as part of the ACE-Asia experiment sampled in similar regions in the Yellow Sea. For example, on 12 April 2001 (ACE-Asia flight 7), a plume largely influenced by biosmoke was observed again by a PILS deployed on the C-130. High concentrations of ionic species and high molar ratios of  $\text{NO}_3^-/\text{SO}_4^{2-}$  were observed. In this case, the  $\text{K}^+$  concentration reached 2.7 ppbv. Five day back trajectories also showed a similar pattern as those of Figure 8 (K. Maxwell-Meier et al., manuscript in preparation, 2003). Other mixed urban/biosmoke plumes were also intercepted during the ACE-Asia study in the Yellow Sea and the Sea of Japan. All these plumes have similar inorganic particulate chemical characteristics, and based on back trajectories, all originate from similar regions.

### 3.5. Associations Between Biomass Burning Aerosols and Relevant Gases

[38] To quantify the characteristics and the relative contribution of biosmoke in the observed Asian outflow during TRACE-P, measurements that were apparently influenced to some extent by biomass or biofuel burning are selected for more detailed analysis. This data set collects measurements from all P-3B research flights from plumes with at least five continuous measurements of  $\text{K}^+$  above the PILS LOD, and with a plume maximum  $\text{K}^+$  concentration higher than 200 pptv. Pollution plumes, with or without  $\text{K}^+$  present, are identified with the same criteria except that  $\text{SO}_4^{2-}$  is used as the criteria species instead of  $\text{K}^+$ . This analysis results in the identification of nine separate plumes with evidence of

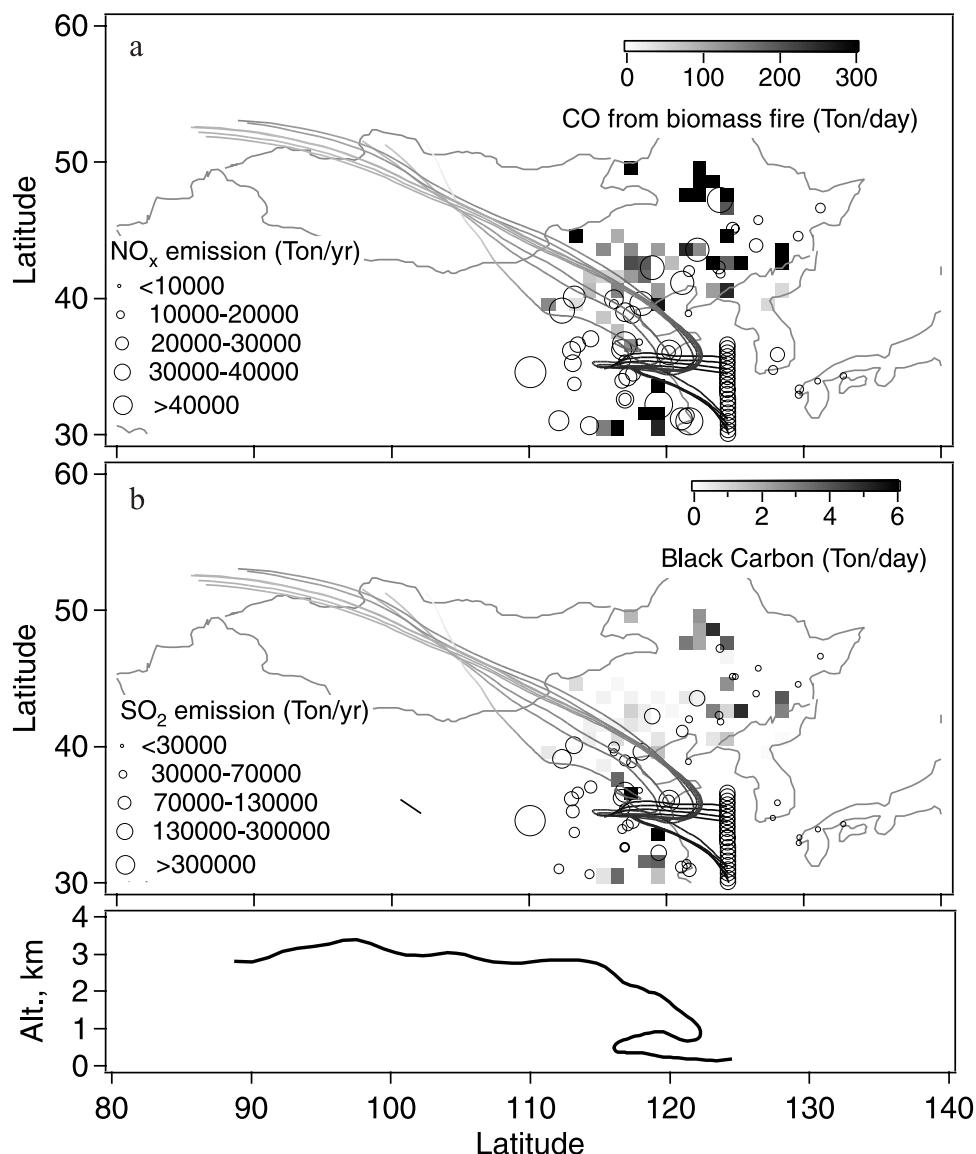


**Figure 8.** (a) Spatial distribution of biomass burning CO and black carbon emissions averaged over 5 days prior to P-3B flight 14 and (b) 5 day back trajectories for the plumes encountered during flight 14. Anthropogenic SO<sub>2</sub> and NO<sub>x</sub> emission sources for 2000 are also shown.

biomsmoke out of a total of 53 plumes measured by the P-3B and produces a data set of 153 points (each a 4 min average) for the biomsmoke plumes. Thus, based on K<sup>+</sup> as a biomsmoke trace, approximately 20% of all the plumes intercepted by the P-3B in TRACE-P indicated some influence from biomass/biofuel burning. Of the plumes containing K<sup>+</sup>, 56% of the measurements were made above 25°N latitude (5 out of the nine plumes), regions where most of the K<sup>+</sup> is possibly from biofuel combustion. Since the aircraft speed is typically 140 m/s, the average scale for the selected plumes is at least 160 km wide.

[39] For this selected data set the following is observed: K<sup>+</sup> has the highest correlation with NH<sub>4</sub><sup>+</sup> ( $r^2 = 0.83$ ) and light-absorbing aerosols (EC) ( $r^2 = 0.80$ ); K<sup>+</sup> is fairly well correlated with CO ( $r^2 = 0.75$ ) and NO<sub>3</sub><sup>-</sup> ( $r^2 = 0.72$ ); K<sup>+</sup> has little correlation with SO<sub>4</sub><sup>2-</sup> with a  $r^2$  of 0.33, and no correlation was observed between K<sup>+</sup> and Na<sup>+</sup>, Cl<sup>-</sup>, or Ca<sup>2+</sup> ( $r^2 = 0.009, 0.011, 0.048$ , respectively) suggesting that

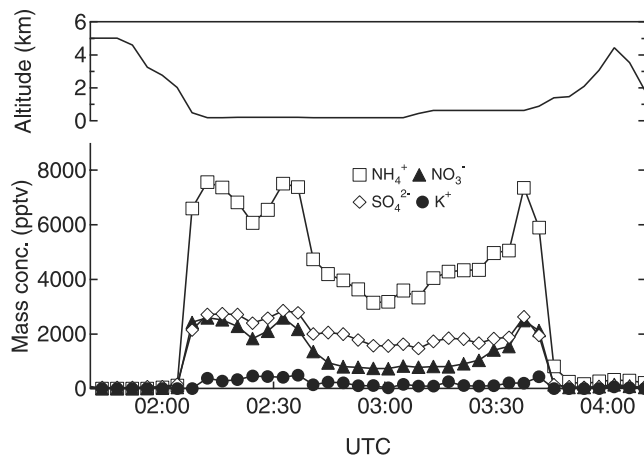


**Figure 9.** Aircraft altitude and fine-particle ionic composition in the Sea of Japan plume of P-3B flight 19.

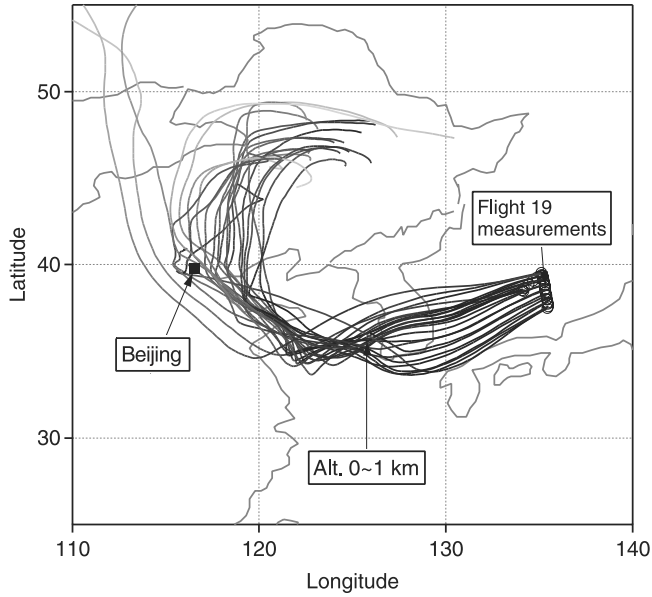


**Figure 10.** The 5 day back trajectories for the plume encountered during flight 19.

the fine potassium was not associated with sea salt or mineral dust. Note that based on  $\text{Ca}^{2+}$  concentrations, only the flight 16 plume is significantly affected by dust; the others show little or no mineral dust contributions.

[40] Because the source for biosmoke is apparently biomass burning emissions for latitudes below  $25^\circ\text{N}$  and possibly biofuel at latitudes higher than  $25^\circ\text{N}$  (based on a correlations between  $\text{K}^+$  and  $\text{SO}_4^{2-}$  and the lack of evidence for widespread biomass burning based on fire maps), the correlations for plumes north of  $25^\circ\text{N}$  are also studied. The results are similar to those for the overall selected data set except that as expected for biofuel use in an urban area, the  $r^2$  for  $\text{K}^+ - \text{SO}_4^{2-}$  increases to 0.44. These results suggest the some form of biosmoke was a significant source of fine-particle  $\text{K}^+$ ,  $\text{NH}_4^+$ , and  $\text{NO}_3^-$ , and also CO and light-absorb-

**Table 2.** Results From Linear Regression Analysis for the Correlation Between Various Fine-Particle and Gaseous Species for the Three Special Plumes Discussed in Detail in the Text<sup>a</sup>

	Flight 10	Flight 14	Flight 19
$\text{SO}_4^{2-}$			
$\text{SO}_4^{2-} + \text{SO}_2$	0.89	0.42	0.51
$\frac{d\text{K}^+}{d\text{CO}}$	2.0 <sup>b</sup>	4.6	2.2
$\frac{d\text{CH}_3\text{Cl}}{d\text{CO}}$	0.87	0.27	0.33
$\frac{d\text{C}_2\text{Cl}_4}{d\text{CO}}$	-0.020	0.0075	0.074
$\frac{d\text{SO}_2}{d\text{CO}}$	0.42 <sup>b</sup>	10	12
$\frac{d\text{SO}_4^{2-} + d\text{SO}_2}{d\text{CO}}$	3.7 <sup>b</sup>	19	26
$\frac{d\text{K}^+}{d\text{SO}_4^{2-}}$	2.4	0.49	0.16
Biomass burning contribution, %	100	$62 \pm 10$	$19 \pm 2$

<sup>a</sup>Units in pptv/ppbv for  $dX/d\text{CO}$  ( $X = \text{K}^+$ ,  $\text{CH}_3\text{Cl}$ ,  $\text{C}_2\text{Cl}_4$ ,  $\text{SO}_2$ ,  $\text{SO}_4^{2-}$ ) and in pptv/ppbv for others.

<sup>b</sup>Low  $r^2$ ; the ratio is calculated as  $\Sigma(X/\text{CO})/n$ .

ing aerosol (EC) in the mixed urban/industrial plumes advecting from Asia.

[41] To investigate the properties of the biosmoke emissions in the TRACE-P data set, and to compare them with findings from other studies, ratios of specific compounds are calculated. The results are summarized in Table 1 for all TRACE-P data, and in Table 2 for the three specific flights discussed above. To minimize the influence of background concentrations, the difference between plume and background concentrations ( $\Delta$ ) is used in the following analysis. After comparing the ratios, this data is used to estimate the contribution of biosmoke to the TRACE-P mixed plumes.

### 3.5.1. $\text{K}^+/\text{CO}$ Ratios

[42] Fine-particle  $\text{K}^+$  emission rates for specific biosmoke plumes can be estimated from  $\text{K}^+/\text{CO}$  ratios. In aged biomass burning plumes, the ratio can also provide a measure of the extent of wet deposition of the fine particles since the  $\text{K}^+$  is removed more efficiently than the CO. However, in plumes of mixed biomass - fossil fuel burning the  $\text{K}^+/\text{CO}$  ratio could be much lower due to additional fossil fuel sources for CO.

**Table 1.** Results From Linear Regression Analysis of the Correlation Among Ambient Aerosol Components and Gas Species for This and Other Studies<sup>a</sup>

	This Work				Other Measurements
	Overall <sup>b</sup>	Maximum	Minimum	Average <sup>c</sup>	
$\frac{d\text{K}^+}{d\text{CO}}$	3.67	4.55 (flight 14)	1.38 (flight 19)	2.86	1.3–4.9, biomass burning, field [Andreae et al., 1988, 1996]; 2.9, Indian Ocean, field [Reiner et al., 2001]
$\frac{d\text{CH}_3\text{Cl}}{d\text{CO}}$	0.33	0.88 (flight 10, 16)	0.22 (flight 19)	0.47	$0.95 \pm 0.01$ , southern Africa, field [Andreae et al., 1996]; $0.85 \pm 0.06$ , Brazilian emissions, field [Blake et al., 1996]
$\frac{d\text{K}^+}{d\text{CO}_4^{2-}}$	0.24	2.37 (flight 10)	0.15 (flight 16, 19)	0.55	0.153, India field [Novakov et al., 2000] <sup>d</sup> ; 0.181, Indian Ocean field [Reiner et al., 2001] <sup>d</sup> ; 4.639, Brazil biomass burning fires [Ferek et al., 1998] <sup>d</sup>
$\frac{d\text{SO}_2}{d\text{CO}}$					
$\frac{d\text{SO}_2}{d\text{CO}}$	9.98	20.05 (flight 14)	0.33 (flight 10)	8.33	$d\text{SO}_2/d\text{CO} = 6.5$ , biomass burning fire, laboratory [Crutzen and Andreae, 1990]; $d\text{SO}_2/d\text{CO} = 4.0$ , biomass burning, field [Andreae et al., 1996]
$(d\text{SO}_2 + d\text{SO}_4^{2-})/d\text{CO}$	17.42	37.48 (flight 16)	3.65 (flight 10)	17.17	$d\text{SO}_2/d\text{CO} = 0.77$ , biomass burning, field [Lacaux et al., 1995]; $d\text{SO}_2/d\text{CO} = 2.4$ – $6.5$ , biomass burning, field [Andreae et al., 1988]; $d\text{SO}_2/d\text{CO} = 7.8$ , $d\text{SO}_4^{2-}/d\text{CO} = 16$ , Indian Ocean field [Reiner et al., 2001]

<sup>a</sup>Units in pptv/ppbv for  $d\text{K}^+/d\text{SO}_4^{2-}$  and in pptv/ppbv for others.

<sup>b</sup>Calculated by the whole selected biosmoke plumes data set.

<sup>c</sup>Average of the corresponding ratios for all selected individual plumes.

<sup>d</sup>Calculated based on the data provided in the paper.



[43] Ambient measurements of  $K^+/CO$  in other studies of pure biomass burning plumes generally are in the range of 1.3–4.9 [Andreae et al., 1988, 1996; Reiner et al., 2001]. The TRACE-P measurements are also in this range (1.4–4.6). Derived from the linear regression slope, for TRACE-P plumes containing some level of  $K^+$ ,  $dK^+/dCO$  molar ratios range from 1.38 to 4.55 pptv/ppbv. The overall average  $dK^+/dCO$  ratio for all TRACE-P plumes with  $K^+$  is 3.67 pptv/ppbv, and the “pure” biomass burning plume of flight 10 has a ratio of 2.02. A summary of comparisons is provided in Table 1. Interestingly, both the mixed plumes of flight 14 and 19 have higher ratios (see Table 2) than the biomass burning plume (flight 10). If the  $K^+$  emission rates are similar for biomass and biofuel burning, then lower ratios are expected in the mixed plumes due to other urban CO sources. This may suggest that more  $K^+$  was lost in the long-range transport prior to detection in the pure biomass burning plume of flight 10 compared to the mixed plumes, or that the emission rates of  $K^+$  are higher in biofuel plumes, the former seems more possible.

### 3.5.2. $dCH_3Cl/dCO$

[44] This ratio has been used as a biomass burning indicator in previous airborne studies [Blake et al., 1999]. In TRACE-P, we recorded  $dCH_3Cl/dCO$  ranging from 0.2 to 0.88 pptv/ppbv (Tables 1 and 2), with the highest value from flight 10, the purest biomass burning plume. The mixed plumes of flights 14 and 19 had ratios of 0.27 and 0.33, respectively. Other studies report  $dCH_3Cl/dCO$  for fresh pure biomass burning smoke in the range of 0.8–1.1 pptv/ppbv [Andreae et al., 2001] and results from other studies are shown in Table 1. Although the TRACE-P data for  $CH_3Cl/CO$  is consistent with other studies, it is again noted, as discussed above, that the correlations between  $CH_3Cl$  and CO are generally low when all the data from different plumes are grouped, and the best correlations are in the relatively pure biomass burning plumes measured in the more southern latitudes (less than 25°N).

### 3.6. Estimates of the Contribution of Biomsmoke Combustion to the Trace-P Plumes ( $K^+/SO_4^{2-}$ , $SO_2/CO$ , and $C_2Cl_4/CO$ )

[45] To estimate the contribution of biosmoke to the measured Asian outflow, we employ a technique used in previous studies based on  $SO_2/CO$  or  $SO_y/CO$  ratios, and investigate the use of fine-particulate  $K^+/SO_4^{2-}$  for estimating the biosmoke contributions to the inorganic fine-particle mass in mixed plumes. In the following analysis, specific ratios are determined from linear regressions.

[46] The justification for the use of these ratios is as follows.  $SO_2/CO$  can serve as an indicator for the lack of biosmoke since in the absence of volcanic emissions,  $SO_2$  is mainly from anthropogenic burning of fossil fuel, with only minor contributions from biomass burning [Chin et al., 1996], and CO is produced from both biomass burning and inefficient fossil fuel combustion. Thus higher  $SO_2/CO$  (or  $SO_y/CO$ ) values indicate less influence from biosmoke. Since  $K^+$  is mainly from biosmoke and  $SO_4^{2-}$  from fossil fuel combustion, the  $K^+/SO_4^{2-}$  ratio should be highest in plumes of greater biosmoke influence. (Note, this will not apply to other regions with additional sources of fine water-soluble particulate  $K^+$ ).

[47] In TRACE-P,  $dSO_2/dCO$  range from 0.33 to 20.05 pptv/ppbv. The overall ratio for plumes with some biomass/biofuel burning is 9.98 pptv/ppbv. For relatively pure biomass burning emissions from previous field and laboratory studies, typical  $dSO_2/dCO$  ratios are between 2 and 5 pptv/ppbv, which are consistent with our measurements (Table 1). The ratio of  $dSO_2/dCO$  can also be determined from emission inventories (in this case the ratio is  $SO_2/CO$ ). Formenti et al. [2002] reports a  $SO_2/CO$  molar ratio for fossil fuel pollution in eastern Europe of 50 pptv/ppbv. Streets and Waldhoff [1998, 1999] give a ratio of 42 pptv/ppbv for the India emission inventory, and Streets et al. [2003] also reports an Asian  $SO_2/CO$  ratio of 54 pptv/ppbv based on anthropogenic emission inventories.

[48] The ratio of total sulfur to CO,  $(dSO_4^{2-} + dSO_2)/dCO$ , is preferred since at times  $SO_4^{2-}$  can comprise a large portion of the total sulfur; TRACE-P sulfate can account for as high as 89% of the total sulfur (shown in Table 2). In general  $(dSO_4^{2-} + dSO_2)/dCO$  ratios range from 3.65 to 37.48 pptv/ppbv, and the overall ratio for all plumes with some biomass burning is 17.17 pptv/ppbv. This value is similar to the ratio reported by Reiner et al. [2001] for a mixed plume over the Indian Ocean (see Table 1).

[49] The TRACE-P  $dK^+/dSO_4^{2-}$  ratios range from the highest, 2.37 pptv/pptv (“pure” biomass burning plume, flight 10), to the lowest of 0.16 pptv/pptv (flight 19). The overall ratio for the TRACE-P data set having evidence of biomass/biofuel burning is 0.24 pptv/pptv, which is comparable to other studies that report 0.15 pptv/pptv [Novakov et al., 2000] and 0.18 pptv/pptv [Reiner et al., 2001] for measurements made during the India Ocean Experiment (INDOEX). A ratio of 4.64 pptv/pptv was reported for biomass burning in Brazil [Ferek et al., 1998]. Other ratios can also be used to quantify biosmoke or fossil fuel contributions in plumes. For example,  $C_2Cl_4$  may serve as a marker for urban/industrial emissions [Blake et al., 1999]. Nearly 93% of  $C_2Cl_4$  is emitted in the Northern Hemisphere [Blake et al., 1999]. Talbot et al. [1996] observed enhancements of  $C_2Cl_4$  downwind of the highly urbanized east coast of Brazil. Thus  $C_2Cl_4/CO$  can provide a scale for urban/industrial influence. This ratio is consistent with our data. As shown in Table 2, it is essentially zero in the pure biomass burning plume of flight 10, and highest in flight 19, the Sea of Japan plume of case 2 that contained relatively low concentrations of  $K^+$ . In contrast, since  $CH_3Cl$  serves as a biomass burning tracer,  $CH_3Cl/CO$  can gauge the influence of biomass burning, however, for this data, poor correlations between  $CH_3Cl$  and CO in the different plumes make this analysis less effective.

### 3.7. Percent Biosmoke Contribution to Trace-P Plumes

[50] Using the ranges of  $dSO_2/dCO$  (or  $dSO_y/dCO$ ), based on measurements and emission inventories of  $SO_2$  and CO, and ratios of  $dK^+/dSO_4^{2-}$ , the relative contribution of biomass/biofuel burning in the various TRACE-P plumes can be estimated. To estimate the percent biosmoke contribution to CO in a plume, a method similar to Formenti et al. [2002] is used. The  $dSO_y/dCO$  molar ratio from fossil fuel emissions (i.e., 0% biosmoke contribution) is assumed to be 40 pptv/ppbv, and for a pure biosmoke plume (i.e., 100% biosmoke contribution) a ratio of 5 pptv/ppbv is assumed. (Note, this accounts for the small amount of  $SO_y$  in

biosmoke plumes). Using these numbers and assuming a linear interpolation between the two extremes, the percent relative influence of biosmoke contribution can be estimated from measured  $d\text{SO}_y/d\text{CO}$  ratios between 5 and 40 pptv/ppbv via the equation; percent biosmoke contribution to  $\text{CO} = 114.29 - 2.86 \cdot (d\text{SO}_y/d\text{CO})$ .

[51] For  $d\text{K}^+/d\text{SO}_4^{2-}$ , we take a similar approach. On the basis of the ranges of  $d\text{K}^+/d\text{SO}_4^{2-}$  observed in TRACE-P and especially in the pure biomass burning plumes observed in flights 9 and 10 ( $d\text{K}^+/d\text{SO}_4^{2-} = 0.81$  and  $2.37$  pptv/pptv, respectively), it is assumed that pure biomass burning plumes have  $d\text{K}^+/d\text{SO}_4^{2-}$  molar ratios equal or larger than  $0.7$  pptv/pptv. For plumes mainly composed of fossil fuel emissions, the minimum ratio of  $d\text{K}^+/d\text{SO}_4^{2-}$  for TRACE-P data is  $0.16$  pptv/pptv. Gabriel *et al.* [2002] report a lower ratio of  $0.07$  pptv/pptv for the aerosols from Arabia with strong influence from fossil fuel. We assume a  $d\text{K}^+/d\text{SO}_4^{2-}$  ratio of less than or equal to  $0.1$  pptv/pptv indicative of plumes having little biosmoke influence (assume 10%). It is again noted that this method is only an estimation of the biosmoke contribution in the mixed plumes since it does not account for the variability in the emission profiles of  $\text{K}^+/\text{SO}_4^{2-}$  for the wide range of plumes investigated in these experiments. However, more rigorous methods for source apportionment involving measurements of emission profiles for specific sources are currently not possible from airborne measurements spanning a large geographical region. The predictions of these two methods using the data from TRACE-P are compared in Figure 11. The data in Figure 11 includes all the selected TRACE-P plumes that were affected by both biosmoke and fossil fuel emissions. Figure 11a shows that as expected,  $d\text{K}^+/d\text{SO}_4^{2-}$  and  $d\text{SO}_y/d\text{CO}$  are inversely related. Applying the linear regressions, Figure 11b shows that the two methods provide fairly similar predictions for the percent contribution of biosmoke. For the most part deviations from the regression line for the two methods are within 20%.

[52] For the five mixed plumes intercepted north of  $25^\circ\text{N}$  latitude during TRACE-P, the percent biosmoke contribution predicted from the  $d\text{K}^+/d\text{SO}_4^{2-}$  ratios is correlated to the measured fine inorganic particle mass concentration, see Figure 12. A similar correlation is also observed with the fine-particle volume (and thus fine-particle mass concentration) measured with an optical particle counter for diameters between  $0.1$  and  $0.75 \mu\text{m}$ , where percent biosmoke to fine-particulate volume  $r^2 = 0.85$ . Thus plumes with higher fine-particle volume (mass) have higher contributions of biosmoke. The fine-particle volume and percent biosmoke based on  $d\text{SO}_y/d\text{CO}$ , which has been used to predict CO contributions from biosmoke [Formenti *et al.*, 2002], are fairly well correlated with an  $r^2$  of  $0.69$  for the mixed plumes intercepted north of  $25^\circ\text{N}$  latitude.

[53] Also plotted in Figure 12 is the measured fine inorganic mass of the plumes lacking biosmoke for latitudes greater than  $25^\circ\text{N}$ . In almost all cases, the mixed urban/industrial and biosmoke plumes have much higher fine-particle concentrations than the pure urban/industrial plumes based on a lack of  $\text{K}^+$ . This suggests that biosmoke, which for this latitude range could be mainly from biofuel, makes significant contributions to the fine-particle concentrations for the TRACE-P regions investigated. It also may reflect the source of the plumes, since plumes with  $\text{K}^+$  are

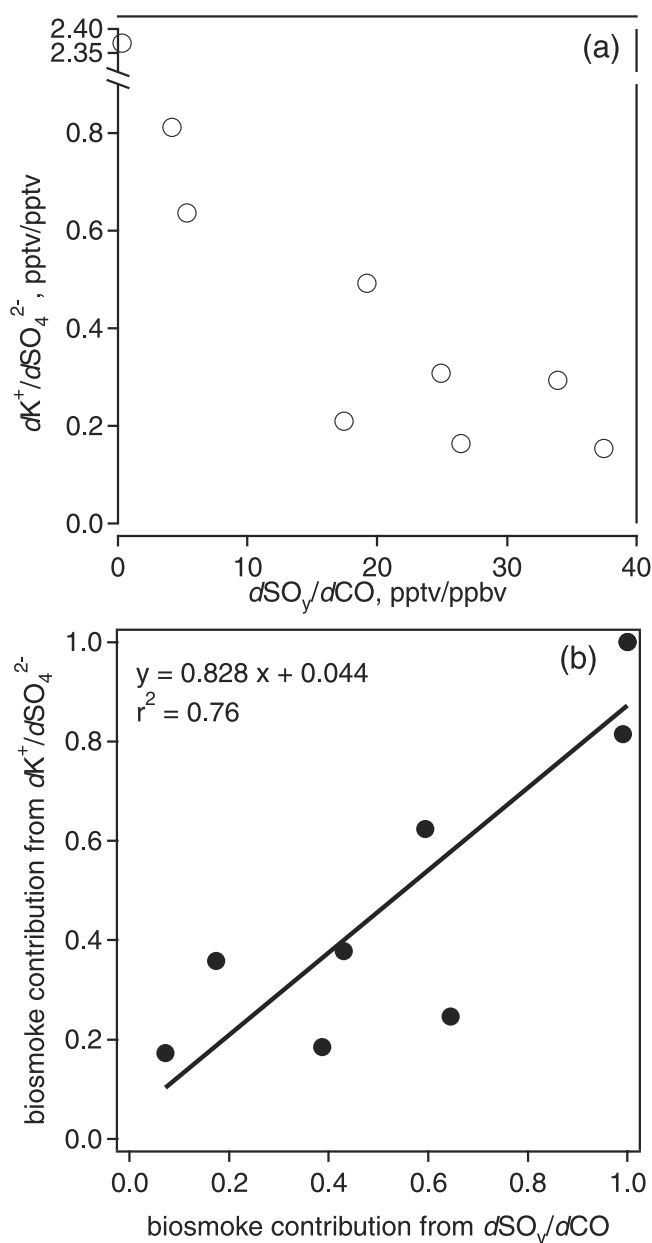


**Figure 11.** (a) Relationship between  $d\text{K}^+/d\text{SO}_4^{2-}$  and  $d\text{SO}_y/d\text{CO}$  and (b) the estimated percent of biosmoke contribution to the mixed urban/biosmoke plumes encountered during TRACE-P based on these two ratios.

apparently associated mainly with emissions from China (see Figure 6) in regions of some of the largest urban/industrial sources.

[54] Applying the linear fit for percent biosmoke based on TRACE-P measurements of  $d\text{K}^+/d\text{SO}_4^{2-}$  to the ACE-Asia data set produces apparently unrealistic results. As shown in Figure 12, predictions of larger biosmoke influence, due to larger ratios of  $d\text{K}^+/d\text{SO}_4^{2-}$ , are correlated with much lower total ionic mass concentrations. This difference may be due to the very high concentrations of mineral dust in the ACE-Asia plumes (K. Maxwell-Meier *et al.*, manuscript in preparation, 2003), which may affect the  $d\text{K}^+/d\text{SO}_4^{2-}$  ratio. For example, in the dust plumes reactions between dust and

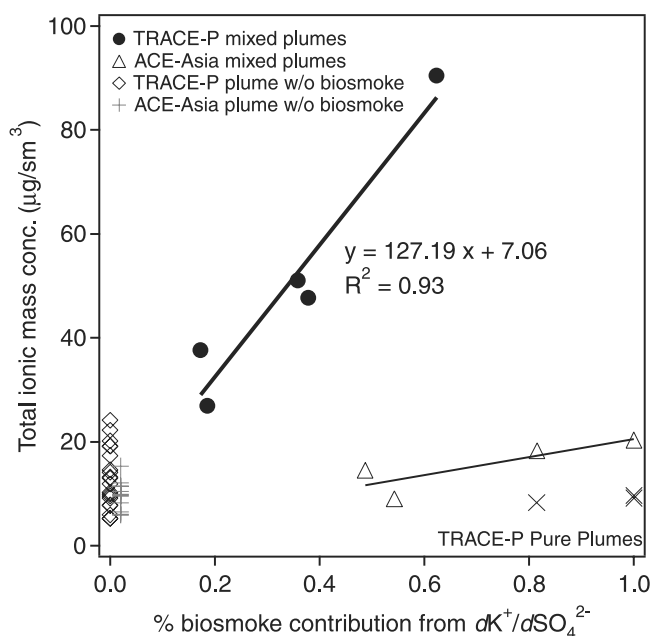


**Figure 12.** Correlation between the percent biosmoke contribution in the mixed urban/industrial and biosmoke plumes and the measured fine-particulate inorganic mass concentration (total measured ionic mass –  $\text{Ca}^{2+}$  –  $\text{Mg}^{2+}$ ) for the plumes intercepted above  $25^\circ\text{N}$  latitude during TRACE-P. TRACE-P plumes without evidence of biosmoke encountered above  $25^\circ\text{N}$  latitude, pure biomass burning plumes intercepted at lower latitudes, and results from ACE-Asia are also plotted.

urban/industrial pollutants can produce coarse-mode calcium sulfate, which could reduce fine-mode  $\text{SO}_4^{2-}$  in a mixed plume of urban, biomass, and dust and lead to a higher  $dK^+/d\text{SO}_4^{2-}$  ratio. Mineral dust also contains  $K^+$ , however, the PILS measurement of fine water-soluble  $K^+$  do not appear to be significantly influenced by dust contributions (K. Maxwell-Meier et al., manuscript in preparation, 2003). Note that in Figure 12, mineral dust contributions to the total fine ionic mass (calcium and magnesium) have not been included.

[55] A map showing the location of the plumes and percent contribution from biosmoke is shown in Figure 13 for TRACE-P plumes that contain some evidence for biosmoke (based on  $K^+$ ). Also marked on the map is the location of plumes with evidence of biosmoke, based on fine-particle  $K^+$ , measured in ACE-Asia. The percent biosmoke is not given for these plumes. The “pure” plumes with 100% biosmoke are located at the lower latitudes of the regions investigated in TRACE-P, which back trajectories show are apparently from wide spread biomass burning emissions in Southeast Asia (see Figure 1). The mixed pollution/biosmoke plumes that contain less than 100% biosmoke are mostly observed at the higher latitudes. On the basis of  $dK^+/d\text{SO}_4^{2-}$  and  $d\text{SO}_y/d\text{CO}$  ratios, on average, the biosmoke contribution in these mixed plumes is predicted to be from 35 to 40%, respectively. For the two case studies discussed above, flights 14 and 19, both ratios predict approximately a 60% biosmoke contribution for flight 14, and a 20–40 % contribution for flight 19, based on  $dK^+/d\text{SO}_4^{2-}$  and  $d\text{SO}_y/d\text{CO}$ , respectively.

[56] For plumes intercepted north of  $25^\circ\text{N}$  latitude, most of the back trajectories for the plumes that were partially composed of biosmoke, indicated by  $K^+$ , passed through the corridor identified by the solid line in Figure 13, while the back trajectories for all the plumes (based on  $\text{SO}_4^{2-}$ ) originated from a much broader range indicated by the dotted line in Figure 13. It is noted that pollution plumes can also pass through the solid line region without any biosmoke signature. The region indicated by the solid line encompasses the large urban centers of Beijing and Tianjin. On the basis of satellite fire map data for latitudes above  $25^\circ\text{N}$ , widespread biomass burning emissions in these regions are low. Thus it is possible the observed biosmoke is due to biofuel use and not due to significant open field biomass burning. This is further supported by the fact that all plumes with evidence for biosmoke above  $25^\circ\text{N}$  latitude were mixed with fossil fuel emission tracers, whereas below this latitude the biosmoke plumes were not.

#### 4. Summary

[57] In Asian outflow plumes measured from the NASA P-3B research aircraft during TRACE-P, fine-particle potassium ( $K^+$ ) concentrations serve as a unique tracer for biosmoke. For all research flights conducted from Hong Kong, China, and Yokota Air Force Base, Japan, based on the presence of fine-particle potassium, approximately 20% of the plumes encountered by the P-3B during TRACE-P appear to be influenced to some extent by biosmoke emissions. For all TRACE-P data,  $K^+$  is correlated with

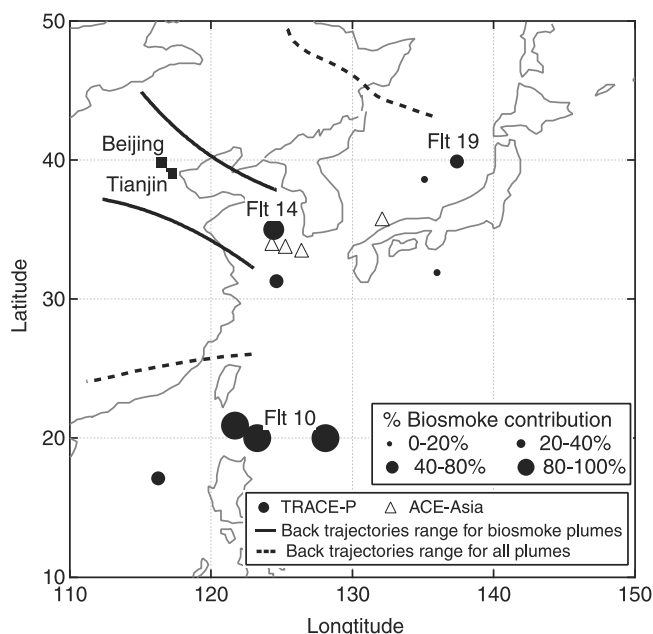


**Figure 13.** Spatial distribution of the estimated percent biosmoke contribution to the mixed urban/biosmoke plumes encountered during TRACE-P. The locations of plumes with evidence of biosmoke during ACE-Asia are also plotted. The solid lines indicate the corridor through which biosmoke plumes intercepted north of  $25^\circ\text{N}$  latitude originated or passed through (based on  $K^+$ ), while the dotted lines indicate the corridor for all plumes intercepted north of  $25^\circ\text{N}$  latitude (based on  $\text{SO}_4^{2-}$ ).



optically absorbing particles ( $r^2 = 0.73$ ), ammonium ( $r^2 = 0.77$ ), and CO ( $r^2 = 0.61$ ). In this study, the  $K^+$  to CO correlation is higher than that between methylchloride ( $CH_3Cl$ ) and CO ( $r^2 = 0.50$ ), a commonly used gaseous biomass burning tracer. No significant correlations between fine  $K^+$  and sodium or calcium indicate that sea salt and mineral dust make little contributions to the observed  $K^+$ .

[58] Purest biomass burning plumes were measured at latitudes between approximately  $15^\circ$  and  $25^\circ N$ , and were found in layers at altitudes from 2 to 4 km asl. Backward trajectories, combined with satellite fire map data suggest that these biomass burning plumes originated from regions of extensive burning in Southeast Asia. In these relatively pure biomass burning plumes, concentrations of fine-particle  $K^+$ ,  $NH_4^+$ ,  $NO_3^-$  and absorbing aerosol particles are all enhanced and correlated.

[59] At latitudes higher than  $25^\circ N$  in regions of Asian outflow, mixed plumes of biosmoke and fossil fuel emissions, based in part on  $K^+$  and  $SO_4^{2-}$  concentrations, were mainly observed in the marine boundary layer. A total of 5 mixed plumes out of 53 were observed at latitude north of  $25^\circ N$  during TRACE-P. During the ACE-Asia experiment, conducted 1 month following TRACE-P, mixed plumes were also observed in similar locations. Back trajectories show that these plumes were associated with air masses that had passed through a fairly narrow latitude range of  $34^\circ$  and  $40^\circ N$  along the eastern China coast, a region that includes the megacities Beijing and Tianjin. A lack of extensive biomass burning in these regions and the high correlation between fossil fuel emissions and biosmoke tracers in these plumes suggest that the biosmoke emissions may be mainly from biofuel.

[60] Molar ratios of fine-particle  $dK^+/dSO_4^{2-}$  and  $SO_2/CO$  are used to estimate the relative influence of biosmoke to the mixed plumes intercepted during TRACE-P. The percent biosmoke contribution to these plumes, based on  $dK^+/dSO_4^{2-}$  ratios, is correlated with the measured fine inorganic aerosol mass ( $r^2 = 0.93$ ) and fine aerosol volume ( $r^2 = 0.85$ ) in the mixed plumes. These mixed plumes were also the most polluted, since the total fine-particle ionic mass and fine volume for plumes with any evidence of biosmoke is generally much higher than plumes lacking biosmoke. The plume composed of the highest fine-particle volume (mass),  $K^+$ ,  $NO_3^-$ ,  $NH_4^+$ , and  $SO_4^{2-}$ , and optically absorbing particles (i.e., soot), and CO of TRACE-P and ACE-Asia was observed in the Yellow Sea. Ratios of  $dK^+/dSO_4^{2-}$  suggest that approximately 60% of the plume was due to biosmoke emissions, the highest contribution of biosmoke to a mixed plume observed in TRACE-P. The results suggest that some form of biosmoke, likely due to the use of biofuel, made significant contributions to the plumes advecting from Asia north of  $25^\circ N$  latitude observed during the TRACE-P and ACE-Asia experiments.

[61] **Acknowledgments.** The authors gratefully acknowledge the support of the National Atmospheric and Space Administration (NASA) under grant number NCC-1-411L. We also thank the personnel of the NASA Wallops Flight Facility for all their help during the experiment.

## References

- Andreae, M. O., Soot carbon and excess fine potassium: Long-range transport of combustion-derived aerosols, *Science*, 220, 1148–1151, 1983.

- Andreae, M. O., and P. Merlet, Emission of trace gases and aerosols from biomass burning, *Global Biogeochem. Cycles*, 15, 955–966, 2001.
- Andreae, M. O., et al., Biomass burning emissions and associated haze layers over Amazonia, *J. Geophys. Res.*, 93, 1509–1527, 1988.
- Andreae, M. O., E. Atlas, H. Cachier, W. R. Cofer III, G. W. Harris, G. Helas, R. Koppmann, J.-P. Lacaux, and D. E. Ward, Trace gas and aerosol emissions from savanna fires, in *Biomass Burning and Global Change*, vol. 1, edited by J. S. Levine, pp. 278–295, MIT Press, Cambridge, Mass., 1996.
- Andreae, M. O., et al., Transport of biomass burning smoke to the upper troposphere by deep convection in the equatorial region, *Geophys. Res. Lett.*, 28, 951–954, 2001.
- Blake, N. J., D. R. Blake, B. C. Sive, T.-Y. Chen, F. S. Rowland, J. E. Collins Jr., G. W. Sachse, and B. E. Anderson, Biomass burning emissions and vertical distribution of atmospheric methyl halides and other reduced carbon gases in the South Atlantic region, *J. Geophys. Res.*, 101, 24,151–24,164, 1996.
- Blake, N. J., et al., Influence of southern hemispheric biomass burning on midtropospheric distributions of nonmethane hydrocarbons and selected halocarbons over the remote South Pacific, *J. Geophys. Res.*, 104, 16,213–16,232, 1999.
- Bond, T. C., T. L. Anderson, and D. Campbell, Calibration and intercomparison of filter-based measurements of visible light absorption by aerosols, *Aerosol Sci. Technol.*, 30, 582–600, 1999.
- Cachier, H., J. Ducret, M.-P. Bremond, Y. Yoboue, J.-P. Lacaux, A. Gaudichet, and J. Baudet, Biomass burning in a savanna region of the Ivory Coast, in *Global Biomass Burning: Atmospheric Climatic and Biospheric Implications*, edited by J. S. Levine, pp. 174–180, MIT Press, Cambridge, Mass., 1991.
- Chin, M., D. J. Jacob, G. M. Gardner, M. S. Foreman-Fowler, P. A. Spiro, and D. L. Savoie, A global three-dimensional model of tropospheric sulfate, *J. Geophys. Res.*, 101, 18,667–18,690, 1996.
- Clarke, A. D., A thermo-optic technique for in situ analysis of size-resolved aerosol physicochemistry, *Atmos. Environ.*, 25, 635–644, 1991.
- Crutzen, P. J., and M. O. Andreae, Biomass burning in the tropics: Impact on atmospheric chemistry and biogeochemical cycles, *Science*, 250, 1669–1678, 1990.
- Dibb, J. E., R. W. Talbot, B. L. Lefer, E. Scheuer, G. L. Gregory, E. V. Browell, J. D. Bradshaw, S. T. Sandholm, and H. B. Singh, Distributions of beryllium 7 and lead 210, and soluble aerosol-associated ionic species over the western Pacific: PEM-West B February–March 1994, *J. Geophys. Res.*, 102, 28,287–28,302, 1997.
- Fang, M., M. Zheng, F. Wand, K. L. To, A. G. Jaafar, and S. L. Tong, The solvent-extractable organic compounds in the Indonesia biomass burning aerosols: Characterization studies, *Atmos. Environ.*, 33, 783–795, 1999.
- Ferek, R. J., J. S. Reid, P. V. Hobbs, D. R. Blake, and C. Lioussie, Emission factors of hydrocarbons, halocarbons, trace gases, and particles from biomass burning in Brazil, *J. Geophys. Res.*, 103, 32,107–32,118, 1998.
- Fine, P. M., G. R. Cass, and B. R. T. Simoneit, Organic compounds in biomass smoke from residential wood combustion: Emissions characterization at a continental scale, *J. Geophys. Res.*, 107(D21), 8349, doi:10.1029/2001JD000661, 2002.
- Formenti, P., et al., The STAAARTE-MED 1998 summer airborne measurements over the Aegean Sea: 1. Aerosol particles and trace gases, *J. Geophys. Res.*, 107(D21), 4550, doi:10.1029/2001JD001337, 2002.
- Frazier, M. P., Z. W. Yue, R. J. Tropp, S. D. Kohl, and J. C. Chow, Molecular composition of organic fine particulate matter in Houston, TX, *Atmos. Environ.*, 36, 5751–5758, 2002.
- Fuehlberg, H. E., R. O. Loring Jr., M. V. Watson, M. C. Sinha, K. E. Pickering, A. M. Thompson, G. W. Sachse, D. R. Blake, and M. R. Schoeberl, TRACE-A trajectory intercomparison: 2. Isentropic and kinematic methods, *J. Geophys. Res.*, 101, 23,927–23,939, 1996.
- Gabriel, R., O. L. Mayol-Bracero, and M. O. Andreae, Chemical characterization of submicron aerosol particles collected over the Indian Ocean, *J. Geophys. Res.*, 107(D19), 8005, doi:10.1029/2000JD000034, 2002.
- Gaudichet, A., F. Echalar, B. Chatenet, J. P. Quisefit, G. Malingre, H. Cachier, P. Buat-Menard, P. Artaxo, and W. Machaut, Trace elements in tropical African savanna biomass burning aerosols, *J. Atmos. Chem.*, 22, 19–39, 1995.
- Heald, C., D. J. Jacob, P. I. Palmer, M. J. Evans, G. W. Sachse, H. Singh, and D. Blake, Biomass burning emission inventory with daily resolution: Application to aircraft observations of Asian outflow, *J. Geophys. Res.*, 108(D21), 8811, doi:10.1029/2002JD003082, in press, 2003.
- Huebert, B. J., T. Bates, P. B. Russell, G. Shi, Y. J. Kim, K. Kawamura, G. Carmichael, and T. Nakajima, An overview of ACE-Asia: Strategies for quantifying the relationships between Asian aerosols and their climatic impacts, *J. Geophys. Res.*, 108(D23), 8633, doi:10.1029/2003JD003550, in press, 2003.
- Jacob, D. J., J. Crawford, M. M. Kleb, V. S. Connors, R. J. Bendura, J. L. Raper, G. W. Sachse, J. Gille, L. Emmons, and J. C. Heald, Transport and



- Chemical Evolution Over the Pacific (TRACE-P) mission: Design, execution, and first results, *J. Geophys. Res.*, 108(D20), 8781, doi:10.1029/2002JD003276, in press, 2003.
- Jordan, C. E., J. E. Dibb, B. E. Anderson, and H. E. Fuelberg, Uptake of nitrate and sulfate on dust aerosols during Transport and Chemical Evolution Over the Pacific, *J. Geophys. Res.*, 108(D21), 8817, doi:10.1029/2002JD003101, in press, 2003.
- Kavouras, I. G., and E. G. Stephanou, Particle size distribution of organic primary and secondary aerosol constituents in urban, background marine, and forest atmosphere, *J. Geophys. Res.*, 107(D8), 4069, doi:10.1029/2000JD000278, 2002.
- Kawamura, K., and F. Sakaguchi, Molecular distributions of water-soluble dicarboxylic acids in marine aerosols over the Pacific Ocean including tropics, *J. Geophys. Res.*, 104, 3501–3509, 1999.
- Kubátová, A., R. Vermeylen, M. Claeys, J. Cafmeyer, and W. Maenhaut, Organic compounds in urban aerosols from Gent, Belgium: Characterization, sources, and seasonal differences, *J. Geophys. Res.*, 107(D21), 8343, doi:10.1029/2001JD000556, 2002.
- Lacaux, J. P., et al., Biomass burning in the tropical savannas of Ivory Coast: An overview of the field experiment Fire of Savannas (FOS/DEC-AFE 91), *J. Atmos. Chem.*, 22, 195–216, 1995.
- Lee-Taylor, J. M., G. P. Brasseur, and Y. Yokouchi, A preliminary three-dimensional global model study of atmospheric methyl chloride distributions, *J. Geophys. Res.*, 106, 34,221–34,233, 2001.
- Ma, Y., R. J. Weber, K. Maxwell-Meier, D. A. Orsini, Y.-N. Lee, B. J. Huebert, S. G. Howell, T. Bertram, R. W. Talbot, J. E. Dibb, and E. Scheuer, Intercomparisons of airborne measurements of aerosol ionic chemical composition during TRACE-P and ACE-Asia, *J. Geophys. Res.*, 108, doi:10.1029/2003JD003673, in press, 2003.
- Mazurek, M. A., and B. R. T. Simoneit, Higher molecular weight terpenoids as indicators of organic emissions from terrestrial vegetation, *ACS Symp. Ser.*, 671, 92–108, 1998.
- Nolte, C. G., J. J. Schauer, G. R. Cass, and B. R. T. Simoneit, Trimethylsilyl derivatives of organic compounds in source samples and in atmospheric fine particles, *Environ. Sci. Technol.*, 36, 4273–4281, 2002.
- Novakov, T., M. O. Andreae, R. Gabriel, T. W. Kirchstetter, O. L. Mayol-Bracero, and V. Ramanathan, Origin of carbonaceous aerosols over the tropical Indian Ocean: Biomass burning or fossil fuels?, *Geophys. Res. Lett.*, 27, 4061–4064, 2000.
- Orsini, D., Y. Ma, A. Sullivan, B. Sierau, K. Baumann, and R. Weber, Refinements to the Particle-Into-Liquid Sampler (PILS) for ground and airborne measurements of water-soluble aerosol composition, *Atmos. Environ.*, 37, 1243–1259, 2003.
- Reiner, T., D. Sprung, C. Jost, R. Gabriel, O. L. Mayol-Bracero, M. O. Andreae, T. L. Campos, and R. E. Shetter, Chemical characterization of pollution layers over the tropical Indian Ocean: Signatures of emissions from biomass and fossil fuel burning, *J. Geophys. Res.*, 106, 28,497–28,510, 2001.
- Sachse, G. W., J. E. Collins Jr., G. F. Hill, L. O. Wade, L. G. Burney, and J. A. Ritter, Airborne tunable diode laser system for high precision concentration and flux measurements of carbon monoxide and methane, *Proc. SPIE Int. Opt. Eng.*, 1433, 145–156, 1991.
- Sakaguchi, F., and K. Kawamura, Identification of 4-oxoheptanedioic acid in the marine environment by capillary gas chromatography-mass spectroscopy, *J. Chromatogr.*, 687, 315–321, 1994.
- Simoneit, B. R. T., A review of biomarker compounds as source indicators and tracers for air pollution, *Environ. Sci. Technol.*, 6, 159–169, 1999.
- Simoneit, B. R. T., W. F. Rogge, M. A. Mazurek, L. J. Standley, L. M. Hildemann, and G. R. Cass, Lignin pyrolysis products, lignans, and resin acids as specific tracers of plant classes in emissions from biomass combustion, *Environ. Sci. Technol.*, 27, 2533–2541, 1993.
- Simoneit, B. R. T., J. J. Schauer, C. G. Nolte, D. R. Oros, V. O. Elias, M. P. Fraser, W. F. Rogge, and G. R. Cass, Levoglucosan, a tracer for cellulose in biomass burning and atmospheric particles, *Atmos. Environ.*, 33, 173–182, 1999.
- Singh, H. B., et al., In situ measurements of HCN and CH<sub>3</sub>CN over the Pacific Ocean: Sources, sinks, and budgets, *J. Geophys. Res.*, 108(D20), 8795, doi:10.1029/2002JD003006, in press, 2003.
- Sive, B. C., Atmospheric NMHCs: Analytical methods and estimated hydroxyl radical concentrations, Ph.D thesis, Univ. of Calif., Irvine, 1998.
- Streets, D. G., and S. T. Waldhoff, Biofuel use in Asia and acidifying emissions, *Energy*, 23, 1029–1042, 1998.
- Streets, D. G., and S. T. Waldhoff, Greenhouse-gas emission from biofuel combustion in Asia, *Energy*, 24, 841–855, 1999.
- Streets, D., et al., An inventory of gaseous and primary aerosol emissions in Asia in the year 2000, *J. Geophys. Res.*, 108(D21), 8809, doi:10.1029/2002JD003093, in press, 2003.
- Tabazadeh, A., M. Z. Jacobson, H. B. Singh, O. B. Toon, J. S. Lin, R. B. Chatfield, A. N. Thakur, R. W. Talbot, and J. E. Dibb, Nitric acid scavenging by mineral and biomass burning aerosols, *Geophys. Res. Lett.*, 25, 4185–4188, 1998.
- Talbot, R. W., et al., Chemical characteristics of continental outflow over the tropical South Atlantic Ocean from Brazil and Africa, *J. Geophys. Res.*, 101, 24,187–24,202, 1996.
- Thornton, D. C., A. R. Bandy, F. H. Tu, B. W. Blomquist, G. M. Mitchell, W. Nadler, and D. H. Lenschow, Fast airborne sulfur dioxide measurements by Atmospheric Pressure Ionization Mass Spectrometry (APIMS), *J. Geophys. Res.*, 107(D22), 4632, doi:10.1029/2002JD002289, 2002.
- Weber, R. J., D. A. Orsini, Y. Duan, Y.-N. Lee, P. J. Klotz, and F. Brechtel, A particle-into-liquid collector for rapid measurement of aerosol bulk chemical composition, *Aerosol Sci. Technol.*, 35, 718–727, 2001.
- Woo, J.-H., et al., Contribution of biomass and biofuel emissions to trace gas distributions in Asia during the TRACE-P experiment, *J. Geophys. Res.*, 108(D21), 8812, doi:10.1029/2003JD003200, in press, 2003.

A. R. Bandy and D. C. Thornton, Department of Chemistry, Drexel University, 32nd and Chestnut Streets, Philadelphia, PA 19104, USA. (bandyar@drexel.edu; thorntdc@drexel.edu)

D. R. Blake, Department of Chemistry, University of California, Irvine, 516 Rowland Hall, Irvine, CA 92697-2025, USA. (drblake@uci.edu)

G. R. Carmichael and J.-H. Woo, Center for Global and Regional Environmental Research, University of Iowa, Iowa City, IA 52242, USA. (gcarmich@icaen.uiowa.edu; woojh21@cgrer.uiowa.edu)

A. D. Clarke, Department of Oceanography, University of Hawaii at Manoa, 1000 Pope Road, Honolulu, HI 96822, USA. (tclarke@soest.hawaii.edu)

H. E. Fuelberg and C. M. Kiley, Department of Meteorology, Florida State University, 404 Love Building, Tallahassee, FL 32306-4520, USA. (fuelberg@met.fsu.edu; ckiley@hucy.met.fsu.edu)

Y.-N. Lee, Environmental Sciences Department, Brookhaven National Laboratory, Upton, NY 11973, USA. (ynlee@bnl.gov)

Y. Ma, K. Maxwell-Meier, D. A. Orsini, and R. J. Weber, School of Earth and Atmospheric Sciences, Georgia Institute of Technology, 221 Boddy Dodd Way, Atlanta, GA 30332, USA. (yma@eas.gatech.edu; kmaxwell@eas.gatech.edu; douglas.orsini@eas.gatech.edu; rweber@eas.gatech.edu)

G. W. Sachse, NASA Langley Research Center, Mail Stop 472, 5 North Dryden Street, Hampton, VA 23681-2199, USA. (g.w.sachse@larc.nasa.gov)

D. G. Streets, Argonne National Laboratory, DIS/900, 9700 South Cass Avenue, Argonne, IL 60439, USA. (dstreets@anl.gov)